activate NF-κB [18,19], which functions in cytokine induction. These studies were mainly performed in mouse macrophages, and results were essentially consistent with other biochemical studies using macrophages [20,21]. Nonetheless, more complicated regulation may occur in other immune-related cells, including mDCs. Recent studies suggested that in mDCs, TLR2 and MyD88 are involved in NK activation that is provoked by bacterial pattern molecules [22,23]. Our previous results also inferred that bacterial lipoproteins act as TLR2 agonists in mDC-driven NK activation [24].

In mDCs, a subset of the antigen-presenting cells, the two major arms of the innate immune signaling pathway, the MyD88 and TICAM-1 (TRIF) pathways, function in the TLR signaling [18,19]. In addition, cytokines including IL-12, IL-15 and IFN-α/β, as well as DC-NK contact are involved in NK cell activation [25,26]. TLR3 is a sensor of dsRNA and induces mDC maturation via TICAM-1 [4,25]. A characteristic feature of TLR3-TICAM-1-mediated mDC maturation is liberation of IL-12, and, independent of IL-12, drives NK cell activation [4]. On the other hand, what factors participate in TLR2-MyD88-mediated mDC maturation to drive NK activation remains largely unknown.

We identified lipopeptides from Triton X-114-solubilized *S. aureus* cells [27,28]. Since *S. aureus* lacks lipoprotein N-acyltransferase, these lipoproteins are predicted to be S-[2,3-bis(palmitoyl)-propyl]cysteines (Pam2Cys) [29]. Their diacylated structure was confirmed by MS/MS spectrometry [28]. We annotated these lipoproteins by function, which largely depends on their protein sequence [30]. Based on these results, we chemically synthesized 16 Pam2Cys lipopeptides of 6–18 amino acids (a.a.) [30]. They possessed TLR2 agonistic activity, but varied in their functional potential to activate NF-κB and liberate TNF-α from human PBMC [30], yet their NK activation potential has not been determined.

This study shows that naïve NK cells are usually in a resting state, and bacterial lipoproteins trigger mDC-mediated NK activation in response to TLR2-derived cellular events. We found that mDC maturation and NK activation are strongly modulated by the amino acid (a. a.) sequence of TLR2 agonistic lipopeptides.

Results

Cytokines liberated from BMDC in response to Pam2 peptides

We synthesized 16 Pam2Cys-containing lipopeptides using *S. aureus* lipoproteins as a reference [30], and designated them Pam2Cys1-Pam2Cys16 (Table 1). Included as positive controls were the diacyl lipopeptides Pam2CSK4 [31], designated as Pam2CSK19 in this study, and its derivatives Pam2CSK (Pam2Cys17), and Pam2CSK2 (Pam2Cys18). Pam2Cys17 was used as a negative control, since this diacyl lipopeptide has virtually no cytokine-inducing activity (Fig. 1). ELAM-luciferase reporter assays were used to assess the NF-κB activation potential of these lipopeptides at 10–500 nM, and a representative result for 100 nM is in Figure 1A. Pam2Cys18 and 19 showed high reporter activity, but Pam2Cys17 did not (Fig. 1A). A series longer than 3 a. a were essential for TLR2 stimulation. The level of TNF-α liberated from mouse BMDC was largely comparable with that induced by human PBMC (Table 1). Pam2Cys4, Pam2Cys13, Pam2Cys15 and Pam2Cys16 exhibited relatively low NF-kB activation and TNF-α production (Table 1, Fig. 1A).

IL-6 and IL-12p40 levels were determined by ELISA using the supernatant of the media from bone marrow-derived DC (BMDC) culture with the lipopeptides for 24 h. The cytokines were detected at high levels in the cultures with lipopeptides, with the exception of Pam2Cys17, Pam2Cys13, and Pam2Cys16 (Fig. 1B,C). The cytokine contents of wells with BMDCs stimulated with Pam2Cys13 and Pam2Cys16 were as low as the control Pam2Cys17.

Table 1. Pam2 lipopeptides used for this study.

No.	Lipid	Amino acid sequence	TNF-α*
Pam2Cys1	Pam2	CANTRHSESDK	++
Pam2Cys2	Pam2	CGTGGKQSSDK	++
Pam2Cys3	Pam2	CGNGNKSGSDD	++
Pam2Cys4	Pam2	CSNIEIFNAKG	+/−
Pam2Cys5	Pam2	CTTDKKEIKAY	+++
Pam2Cys6	Pam2	CSFGGNHKLSS	++
Pam2Cys7	Pam2	CGSQNLAPLEE	+++
Pam2Cys8	Pam2	CGQDSDQQKDG	+++
Pam2Cys9	Pam2	CGNDDGKDKDG	+++
Pam2Cys10	Pam2	CGNNSSKDKEA	+++
Pam2Cys11	Pam2	CSLPGLGSKST	+++
Pam2Cys12	Pam2	CSTSEVIGEKI	++
Pam2Cys13	Pam2	CPFNCVGCYNK	+/−
Pam2Cys14	Pam2	CGSQNLAPLEEK	+/−
Pam2Cys15	Pam2	CLILIIASETL	+/−
Pam2Cys16	Pam2	CLILIIASETLFSFSHLTDVK	+/−
Pam2Cys17	Pam2	CSK	n.d.
Pam2Cys18	Pam2	CSKK	n.d.
Pam2Cys19	Pam2	CSKKKK	++

*100 pg/ml of Pam2 peptides were used for stimulation of PBMC.
TNF-α levels: +/−; <200, ++; 2,000–4,000, +++; 4,000–7,000 pg/ml.
n.d., not determined.
doi:10.1371/journal.pone.0012550.t001

The degree of CD86 upregulation by the 16 *S. aureus* lipopeptides was examined, and similar DC maturation profiles were obtained by flow cytometer for all Pam2Cys tested (Fig. 1D), suggesting BMDC maturation, as determined by CD86 up-regulation, was independent of NF-kB activation or cytokine liberation by these lipopeptides.

NK activation by Pam2Cys peptides

Previous reports suggested that TLR2 agonists can induce NK activation [22–24]. To investigate whether the *S. aureus* lipoproteins had NK cell-activating activity, we added the Pam2Cys peptides at 100 nM to BMDC/NK cultures as described previously [4]. Three markers for NK activation [26] were assessed: IFN-γ production, up-regulation of NK surface markers, and target B16D8 cell cytotoxicity by NK cells (Fig. 2). IFN-γ was generated in the supernatants (sup) in response to the lipopeptides (Fig. 2A). However, Pam2Cys13, Pam2Cys15, and Pam2Cys16 showed significantly low potential for IFN-γ induction as comparable to Pam2Cys17. Cytotoxic activity was evaluated using B16D8 cells as a target [4]. Again, Pam2Cys13, 15 and 16 did not induce effective killing (Fig. 2B). The other *S. aureus* lipopeptides had sufficient killing activity: two simultaneously generated examples are shown in Figure 2B.

The NK cell activation markers CD25 and CD69 were analyzed by flow cytometry after co-culturing NK cells with BMDC and Pam2Cys stimulants (Fig. 2C). Up-regulation of

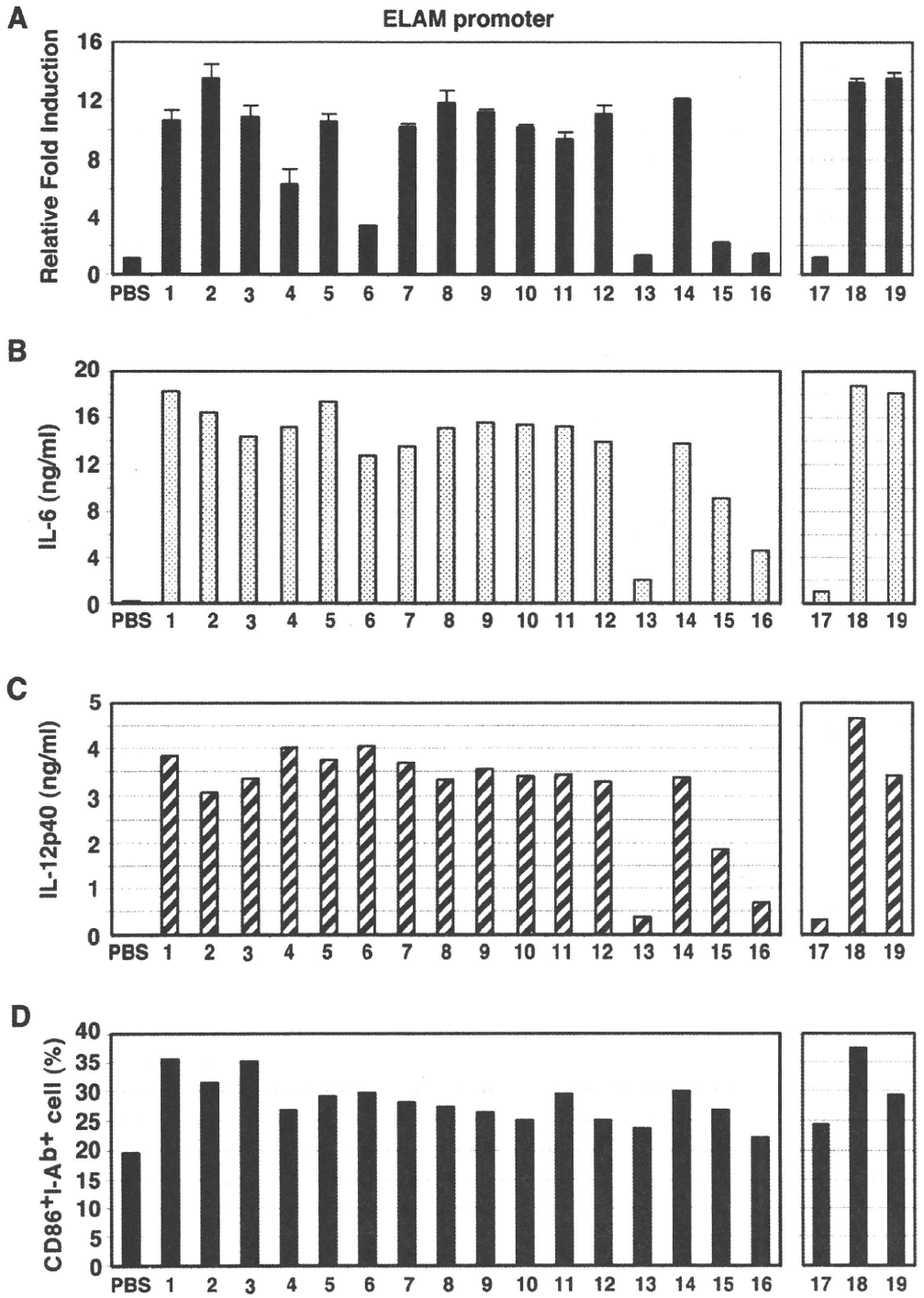

Figure 1. Synthetic Pam2Cys lipopeptides activate TLR2 and induce cytokine production in BMDC. (A) HEK293 cells were transfected with plasmids encoding TLR2 and ELAM-luciferase reporter. After 24 h, the cells were treated with Pam2Cys peptides (100 nM) for 6 h and then luciferase activities of the cell lysates were measured. (B, C) BMDC were treated with Pam2Cys peptides for 24 h and IL-6 and IL-12p40 concentrations in the culture supernatants were measured by ELISA. (D) CD86 and MHC class II (I-Ab) expression of the BMDC were determined by flow cytometry. Data represents the mean ± SD of triplicate measurements. The data shown are representative of at least three independent experiments. The numbers represent the Pam2Cys's numbers.
doi:10.1371/journal.pone.0012550.g001

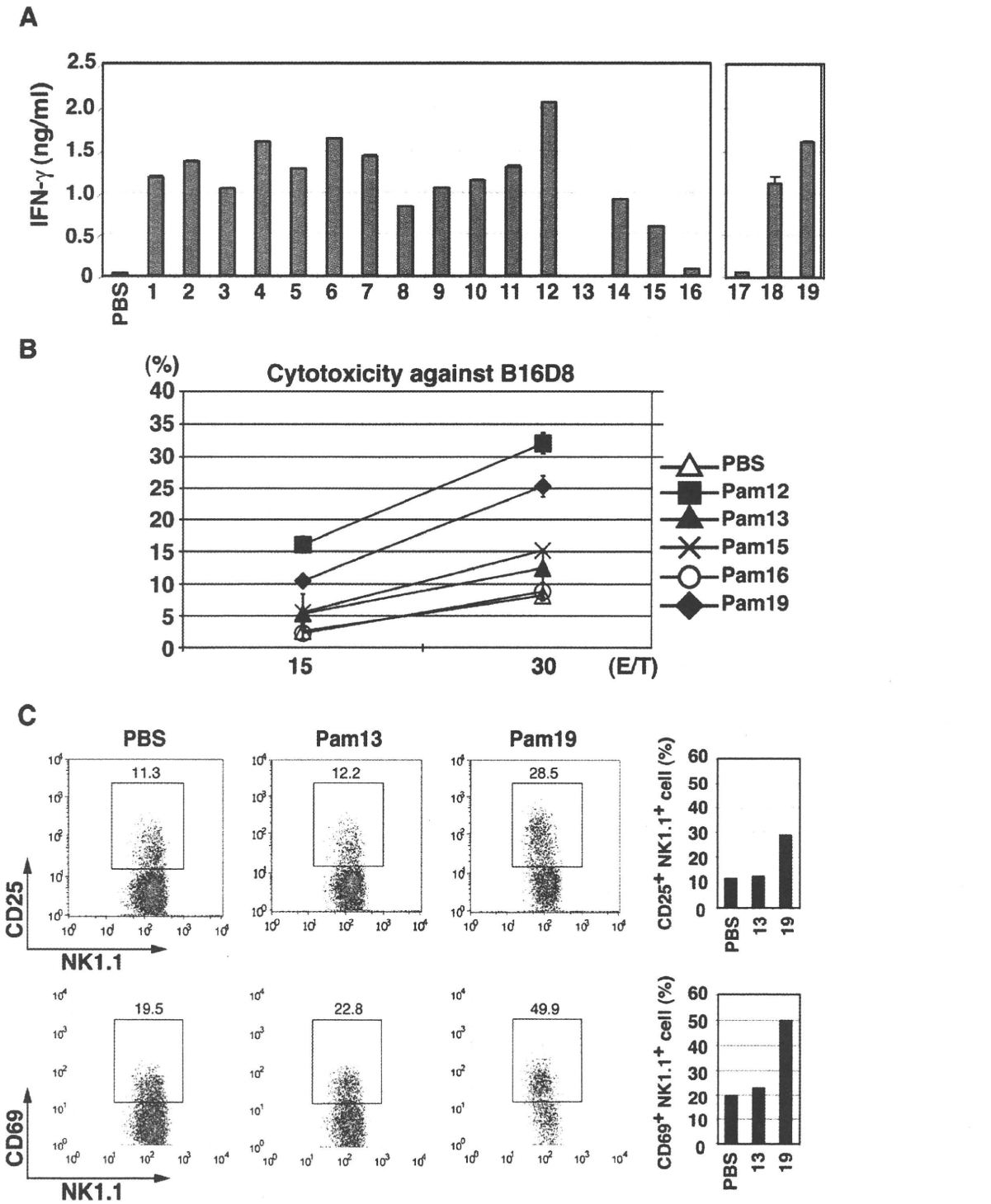

Figure 2. Pam2Cys peptides activate NK cells via BMDC. (A) Wild-type BMDC and wild-type NK cells were co-cultured at 1:2 ratio in the presence of Pam2Cys peptides as the numbers indicated (100 nM). After 24 h, IFN-γ concentrations in the supernatants were measured by ELISA. (B) NK cell cytotoxicity against B16D8 cells was measured by ^{51}Cr release assay at indicated E:T ratios as described in the Methods section. (C) Populations of CD25+ and CD69+ NK cells were measured by flow cytometry after stimulation of NK cells with BMDC treated with indicated Pam2Cys peptides. BMDC were stimulated with control PBS, 100 nM of Pam2Cys13 or Pam2Cys19 for 4 h. Then, BMDC were incubated with NK cells. After 24 h, cells were analyzed by flow cytometer using the markers for separation. %Positive cells are shown to the right.
doi:10.1371/journal.pone.0012550.g002

surface CD25 and CD69 was observed in NK cells incubated with BMDC and Pam2Cys18 or 19, while the levels of their up-regulation by Pam2Cys13, 15 or 16 were near those of the negative control Pam2Cys17, for stimulating NK cells co-cultured with BMDC. In contrast, no increase was observed for CD56, NKp46 and DNAM-1 (data not shown).

Participation of TLR2/MyD88 in Pam2Cys-mediated BMDC and NK activation

Activated NK cells are a major source of IFN-γ, which causes a variety of responses in the immune system. To examine whether direct stimulation of NK cells with Pam2Cys18 or Pam2Cys19 induced secretion of IFN-γ, we measured the frequency of IFN-γ-secreting NK cells, at 24 h after incubation. By intracellular staining, IFN-γ-secreting NK cells were increased after direct Pam2Cys18 or 19 stimulation (data not shown). As shown in Figure 3A and B, TLR2 ligands except Pam2Cys12, 18 and 19 barely increased the levels of IFN-γ of NK cells by co-culture with Pam2Cys-stimulated TLR2−/− or MyD88−/− BMDC. On the other hand, NK cells induce moderate levels of IFN-γ in response to BMDC stimulated with Pam2Cys12, 18 or 19 (open bars in Figure 3A), although no structural similarity was detected between Pam2Cys12 and Pam2Cys18 or 19.

We next examined whether lipopeptide-mediated cytokine secretion and NK activation were dependent on BMDC TLR2 and MyD88. IL-6 and IL-12p40 secretion were completely abrogated in TLR2−/− BMDC (data not shown). However, low amounts of IFN-γ were detected in co-cultures of TLR2−/− or MyD88−/− BMDC and wild-type (WT) NK cells in the presence of Pam2Cys12, 18, or 19 (Fig. 3B,D), and lesser extent of IFN-γ was still detected in co-cultures of WT BMDC and TLR2−/− NK cells in the presence of Pam2Cys12 or Pam2Cys19 (Fig. 3C). These results were reproduced with MyD88−/− BMDC (not shown). Notable results are shown in Fig. 3D where WT or TLR2−/− BMDC were stimulated with indicated Pam2Cys and incubated with WT or TLR2−/− NK cells. Moderate IFN-γ was detected in the media containing TLR2−/− BMDC, WT NK and Pam2Cys12 or 19 (Fig. 3D), the IFN-γ levels being comparable to those of WT NK cells alone stimulated with Pam2Cys12 or 19 (Fig. S1). TLR2−/− NK cells still produced very low levels of IFN-γ when the TLR2−/− NK cells were co-cultured with WT BMDC (Fig. 3D). However, No IFN-γ was detected in the media containing TLR2−/− NK and Pam2Cys12 or 19. Thus, all Pam2Cys peptides including Pam2Cys12, 18 and 19 act on BMDC to drive NK activation. Notably, WT NK cells alone produce minute IFN-γ in response to Pam2Cys12 or 19 (Fig. S1), which means that Pam2Cys12 and Pam2Cys19 additionally induce direct NK activation. The Pam2Cys receptors for this NK activation is through the NK cell TLR2 followed by the MyD88 pathway. However, minute activation by Pam2Cys12 or 18/19 appears to be left in TLR2−/− NK cells stimulated with Pam2Cys12/19-treated BMDC, which should be attributed not to TLR2 but to other unknown mechanisms.

Combinatorial recognition of Pam2Cys lipopeptide by TLR2 and TLR6

TLR2 recognizes diacyl lipopeptides in combination with TLR6 [14,31] while TLR2 recognizes triacyl lipopeptide with TLR1 [15,32]. We found TLR2/6 cooperation in the recognition of *S. aureus* lipopeptides using HEK293 cells that express TLR2/6. Data on the use of TLR2/6 by Pam2Cys12, Pam2Cys13, Pam2Cys15, Pam2Cys16, and Pam2Cys19 is shown in Figure 4. Single receptors of TLR1, TLR6, and TLR10 showed little activation of NF-κB by reporter assay, and only TLR2 exhibited <60-fold ELAM promoter activation (data not shown). Pam2Cys12 and Pam2Cys17 more efficiently activated the ELAM promoter (>300 fold over the control) with TLR2 and 6, than with TLR2 alone (Fig. 4A). TLR1 or TLR10 in combination with TLR2 did not amplify the signal (Fig. 4B). Pam2Cys13 only weakly enhanced the TLR2 potential with additional TLR6 expression in HEK cells (Fig. 4A), and only a slight increase was observed with Pam2Cys15 and Pam2Cys16 with simultaneous expression of TLR2 and TLR6 (Fig. 4A). Hence, TLR6 helped TLR2 to amplify the TLR2 signal from most Pam2Cys lipopeptides, but not with Pam2Cys13 or Pam2Cys15/16.

Critical a.a. in Pam2Cys lipopeptides for BMDC-mediated NK activation

Recent studies revealed an extensive cross-talk between NK cells and mDCs [2,6]. We analyzed the structural background that supports NK activation using our synthetic diacyl lipopeptides. All NK-activating lipopeptides tested had Cys-Ser/Thr or Cys-Gly/Ala in their N-terminus (Table 1). However, the two lipopeptides with the lowest ability to activate NK cells had differences, with Cys-Pro in the N-terminus of Pam2Cys13, and Cys-Leu-Ile in Pam2Cys15/16. When the second Pro in Pam2Cys13 was replaced with Ser, and the Leu-Ile sequence of Pam2Cys16 was replaced with Ser-Asn, the newly synthesized peptides, Pam2-Cys13(P-S) and Pam2Cys16(LI-SN), recovered their ELAM reporter activity (Fig. 5A).

We next tested whether BMDC mature to activate NK cells through BMDC's TLR2 activation by these modified Pam2Cys. Pam2Cys13(P-S) and Pam2Cys15(LI-SN) recovered NK-activating properties by the amino acid conversions judged by IFN-γ production (Fig. 5B) and cytotoxicity against B16D8 cells (Fig. 5C). Since Pam2Cys13(P-S) acts only on BMDC (not shown), this Pam2Cys activity is attributable to recovered BMDC maturation. Hence, Pam2Cys13(P-S) and Pam2Cys16(LI-SN) are NK activators via mDC TLR2. Hence, we conclude that the peptide sequence near the N-terminus is important for NK activation by diacyl lipopeptide.

Production of both IL-6 and IL-12p40 was dependent on BMDC TLR2 (Fig. 6A). Pam2Cys13 and Pam2Cys16 induced these cytokines at very low levels. When Pam2Cys13(P-S) or Pam2Cys16(LI-SN) replaced Pam2Cys13 or Pam2Cys16 in the same assay system, the cytokine levels recovered to levels similar to those of the other lipopeptides (Fig. 6B). These activities were almost completely abrogated in TLR2−/− BMDCs. Thus, the a.a. replacements allows BMDC to generate the TLR2 signal, irrespective of their artificial modifications.

BMDC-NK contact is indispensable for BMDC TLR2-mediated NK activation

Pam2Cys13(P-S) matured BMDC to activate NK cells without direct action on NK cells (Fig. 7A). First, we collected the sup of BMDC stimulated with Pam2Cys13 or Pam2Cys13(P-S). Surprisingly, Both of the sup failed to confer NK activating function on the mixture of naïve BMDC and NK cells (data not shown). The capacity of BMDC sup to induce IFN-γ-secretion by NK cells was further evaluated using a transwell system (Fig. 7A,B). No significant increase in IFN-γ-secreting NK cells was observed when lipopeptide-activated BMDCs and NK cells were separated by transwell (Fig. 7A,B). Frequency of IFN-γ-producing NK cells was high in co-culture with Pam2Cys13(P-S)-stimulated BMDC and NK cells (Fig. 7B upper panel) while the IFN-γ-producing NK

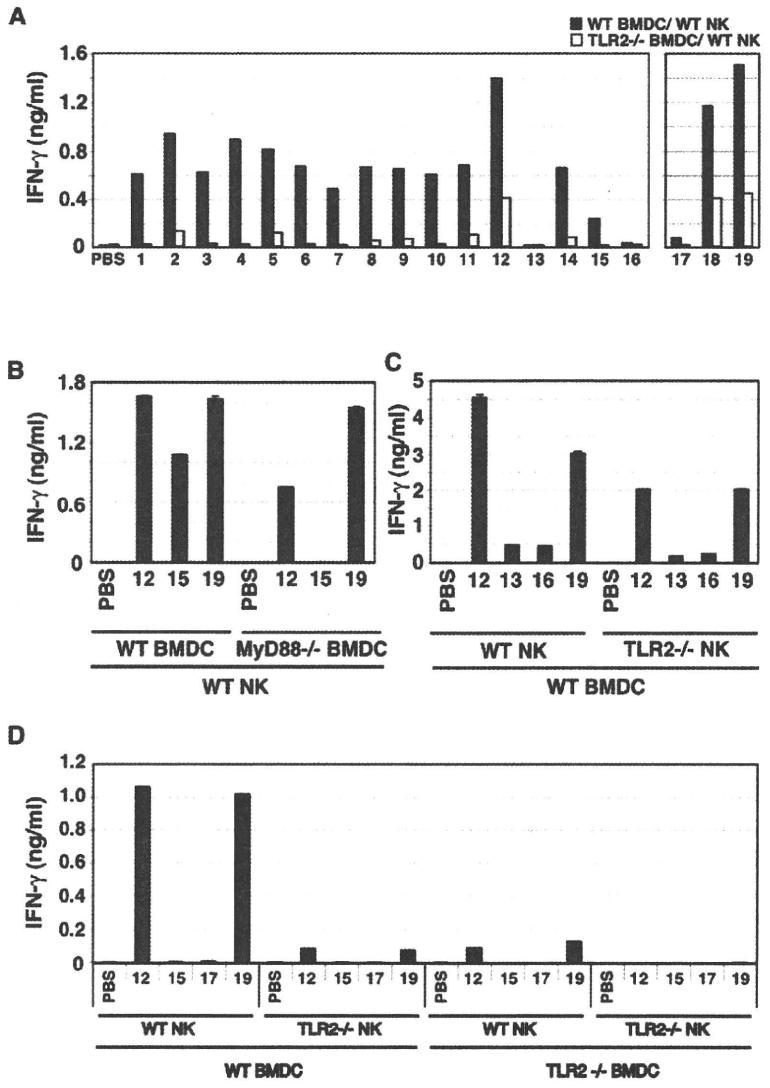

Figure 3. TLR2 on BMDC mainly participate in Pam2Cys-mediated NK activation. (A) BMDC TLR2-independent NK activation by Pam2Cys12, 18 and 19. BMDC from wild-type (closed bars) or TLR2−/− (open bars) mice were stimulated with control PBS or 100 nM of indicated Pam2Cys peptides for 4 h. Cells were then co-cultured with wild-type NK cells at 1:2 ratio for 24 h. Then, the supernatants were collected and IFN-γ was measured by ELISA. (B) Pam2Cys12 and 19 induce NK activation in culture with MyD88−/− BMDC. NK cells were co-cultured with wild-type or MyD88−/− BMDC in the presence of the indicated Pam2Cys peptides (represented by the numbers) as in Fig. 2. 24 h after incubation, culture media were collected to determine cytokines by ELISA. (C) Pam2Cys12 and 19 induce TLR2−/− NK activation in culture with wild-type BMDC. Wild-type BMDC and NK cells with either wild-type or TLR2−/− phenotype were incubated at 1:2 ratio with the indicated Pam2Cys peptides (represented by the numbers) as in Fig. 2. 24 h after incubation, culture media were collected to determine cytokines by ELISA. One representative of the three similar experiments is shown. (D) TLR2 NK cells mainly participates in TLR2 BMDC-independent NK activation by Pam2Cys12 and 19. Wild-type and TLR2−/− BMDC were stimulated with indicated Pam2Cys peptides for 4 h. These BMDC were then mixed with NK cells as shown in the panel. Four groups consisting of either of wild-type NK or TLR2−/− NK and either of wild-type BMDC or TLR2−/− BMDC (see the bottom of the panel) were incubated with the indicated Pam2Cys peptides (50 nM) for 24 h. NK cells alone with Pam2Cys12 or 19 liberated minure IFN-γ as in the panel with WT NK + TLR2−/− BMDC (see Fig. S1). IFN-γ concentrations in the culture supernatants were determined by ELISA. The data shown are representative of at least three independent experiments.
doi:10.1371/journal.pone.0012550.g003

cells were diminished in the transwell (Fig. 7B lower panel). In either case, IL-15 and IFN-α/β were barely increased in Pam2Cys-stimulated BMDCs by RT-PCR (data not shown). Thus, soluble factors barely participate in BMDC-mediated NK activation. BMDC-NK contact is essential for TLR2-mediated NK activation.

Discussion

Here, we demonstrated that the a. a. sequence of *S. aureus* Pam2Cys peptides critically affects the agonistic function for TLR2 and the mode of NK activation. This NK activation is largely dependent on TLR2/MyD88 in BMDC in the mouse

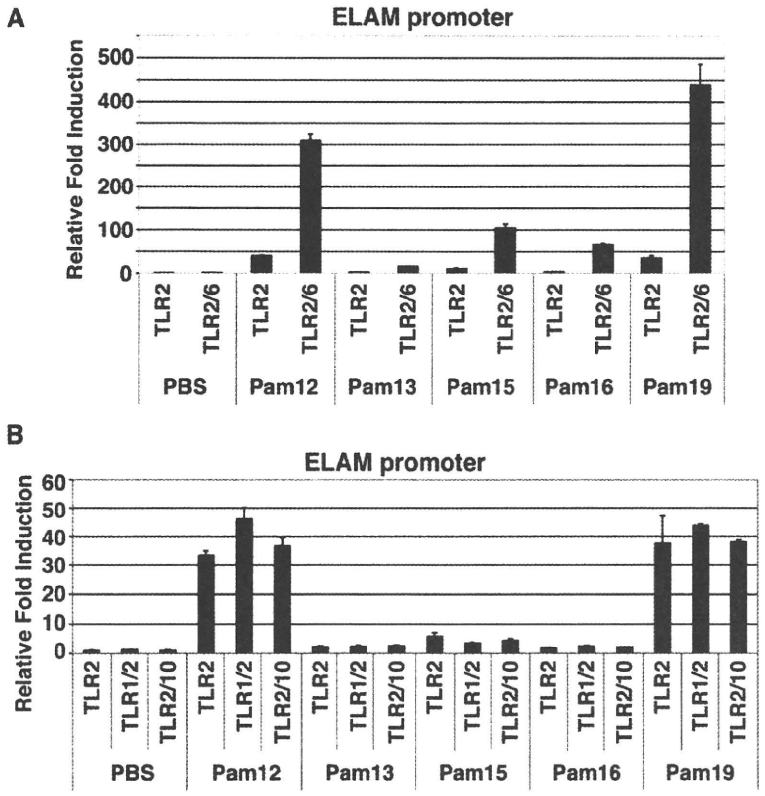

Figure 4. TLR6 promotes TLR2 signaling in Pam2Cys peptides recognition. (A, B) HEK293 cells were transfected with plasmids encoding TLR2, TLR6, TLR1 or TLR10 and the ELAM-luciferase reporter. After 24 h, the cells were treated with indicated Pam2Cys peptides (100 nM) for 6 h and then luciferase activities were measured. The data shown are representative of at least three independent experiments.
doi:10.1371/journal.pone.0012550.g004

system. In addition, Pam2Cys12 and Pam2Cys18/19 have a weak ability to directly activate NK cells without participation of BMDC. In contrast, we determined Pam2Cys13, Pam2Cys15, and Pam2Cys16 to be dysfunctional, since these lipopeptides failed to activate TLR2/6 reporter signaling or induce cytokines in BMDC (Fig. 1,4). Although the first Cys is conserved in all the lipopeptides tested, the following sequences varied, even though all showed BMDC maturation activity. Notably, the second a. a. residue was Ser/Thr or Gly/Ala in the functional lipopeptides, followed by undefined sequences. A length of more than three a.a. was indispensable for BMDC-mediated NK activation (Fig. 1, Pam2Cys17 vs. 18). The failure of Pam2Cys13, Pam2Cys15, and Pam2Cys16 to activate NK cells suggests the importance of the second and/or third residue for stimulating BMDC or directing NK activation. Pam2Cys13 harbors Pro in the second residue, which breaks hydrogen bond interactions. Likewise, Pam2Cys15 and Pam2Cys16 commonly possess Leu and ILe in the second and third residues, which also destabilize hydrogen bond interactions. Thus, these a. a. residues critically influence the effectual interaction between the Pam2Cys peptides and the TLR2 complex on either BMDC or NK cells.

TLR2 initiates immune response by recognizing diacylated lipoproteins in combination with TLR6. We surmise that this receptor complex recognizes the a. a. properties in the peptide sequence that activate mDC/NK cells. Crystal structure analysis indicates that hydrogen bonds between glycerol and the peptide backbone of the ligand and the leucine-rich repeat (LRR)11 loops of TLRs are critical for TLR heterodimerization [31,32]. These hydrogen bonds bridge TLR2 and TLR6 with the ligand, and fix the conformation of the hydrophobic residues around the dimerization interface [31]. The side chains of the first two a. a. of Pam2Cys have substantial interactions with the TLRs. The N-terminal Cys binds to the sulfur site formed by the hydrophobic F325, L328, F349, L350, and P352 residues of TLR2, and the L318 residue of TLR6 [31]. The hydroxyl side chains of the second Ser/Thr form a medium-range hydrogen bond with the F325 backbone of TLR2. As seen in the TLR2/TLR6/Pam2CSK4 structure, the side chains beyond the third lysine residue have highly flexible structures and form only weak ionic or hydrogen bond interactions with the TLRs [31]. Hence, our results with a. a. substitutions fit the proposed TLR2-Pam2CSK4 interacting model.

In a previous report, lysines in the triacyl peptide were seen to form hydrogen bonds with TLRs when Pam3CSK4 interacts with TLR2/TLR1 heterodimer [32]. The ε-amino residues in the side chains appear to participate in lipopeptide recognition by TLRs [31,32]. In our results, the small side chains of Asn or Gly had no blocking effects on the peptide-TLR2 interaction (data not shown). Thus, a hydrophilic or small a. a. in the chain barely altered the lipopeptide function exerted through TLR2. The *S. aureus* lipopeptides, with the exception of Pam2Cys13, Pam2Cys15, and Pam2Cys16 are compatible with this principle. We actually demonstrated here that the peptide sequences have a significant effect on the immunological activity of the lipopeptides. The recognition system for bacterial lipoproteins has developed to

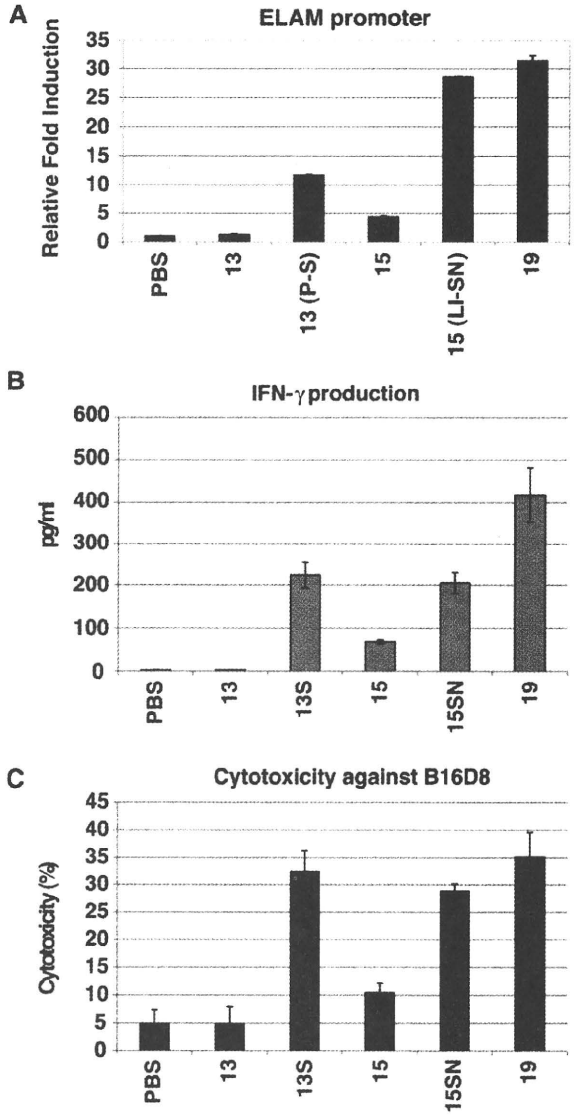

Figure 5. Amino acids near the Pam2 lipid are critical for TLR2 recognition. (A) HEK293 cells were transfected with plasmids encoding TLR2 and the ELAM-luciferase reporter. After 24 h, the cells were treated with indicated Pam2Cys peptides (100 nM) for 8 h and then luciferase activities were measured. The numbers represent the Pam2Cys's numbers. 13(P-S), Pam2Cys13 with second Proline replaced with Serine; 15(LI-SN), Pam2Cys15 with second Leucine and third Isoleucine replaced with Serine and Asparagine. (B,C) BMDC-mediated NK cell activation occurs by stimulation with Pam2Cys13 (P-S) and Pam2Cys15 (LI-SN). BMDC and NK cells were prepared from wild-type mice. BMDC were stimulated with PBS or indicated Pam2Cys peptides for 4 h. Then, BMDC were incubated with wild-type NK cells for 24 h. IFN-γ production (A) and B16D8 cytotoxicity (E:T ratio = 50:1) (B) were measured as in Figure 2. 13S and 15SN represent Pam2Cys13(P-S) and Pam2Cys15(LI-SN), respectively.
doi:10.1371/journal.pone.0012550.g005

sense common structures of the lipid, as well as the peptide sequences.

The factor that determines whether mDC TLR2 or NK TLR2 predominates in diacyl lipopeptide activation has remained to be settled. The sequence information about the NK-activating vs. DC-activating lipopeptides in this study suggests that lysines or hydrophilic a. a distal to Pam2Cys are involved in this selective activity. Peptides with lysines tended to exert direct NK activation. According to the structural studies [31,32], the lysines in Pam3CSK4 form multiple hydrogen bonds with TLR2/1, and the same is expected to be true of Pam2CSK4 and TLR2/6. Hence, hydrophilic residues after the second residue of the Pam2Cys lipopeptides may participate in high affinity interaction with NK cell TLR2/6.

In a previous report, we identified the NK-activating protein INAM, which discriminates between active and resting NK cells, and reflects *in vivo* tumoricidal action of NK cells [33]. INAM is expressed on polyI:C-matured mDCs in response to IRF-3 activation, and is not expressed on mDCs stimulated with TLR2 agonists [33]. In both TLR2- and TLR3-stimulation, IFN-γ is a marker of NK activation [4,6,22,33], almost parallel to NK cell-mediated target cytotoxicity. According to these criteria, mDC drive NK activation via two arrays, MyD88 and TICAM-1 pathways. Anyhow, the MyD88-mediated NK activation occurs independently of TICAM-1-mediated NK activation. Here we provide further knowledge on the MyD88-mediated NK activation: mDC TLR2-dependent, and mDC TLR2-independent pathways exist for NK activation. The latter involves NK TLR2-dependent NK activation, where the lipopeptides directly stimulate TLR2 and the MyD88 pathway in NK cells. However, a minimal NK-activating capacity by Pam2Cys12, 18 and 19 retains in TLR2−/− NK cells. This means that the direct NK activation largely depends on NK cell TLR2/MyD88 but does not neglect participation of other undetermined factors, such as NOD-like receptor (NLR) family, either in mDC or NK cells.

Pam2Cys-matured BMDC produce IL-12 by the MyD88 pathway. Unexpectedly, however, results from transwell studies did not support the importance of IL-12 in NK activation. In addition, NK-activating cytokines, such as IL-15 and IFN-α/β, are barely increased in Pam2Cys-stimulated BMDC (data not shown). Cell-cell contact rather than soluble mediators is crucial for mDC TLR2-mediated NK activation in this study.

Taken together, we showed that *S. aureus* lipopeptides induce mDC-mediated NK activation. It is intriguing that this is a case of the reported reciprocal activation [2], in which ligands-receptors on mDC and NK cells are involved. In a. a. sequences of Pam2Cys, lysine distal to the N-terminal Pam2 and hydroxyl residues proximal to the Pam2 affect NK-activating potential through its interaction with TLR2. When bacteria invade host tissue, they encounter many proteases. Since plasma serine proteases frequently cleave the Lys-X sequence of substrates, the lipoproteins may be clipped out into liberated lipopeptides containing Lys, which could be important in the context of TLR2-induced inflammatory immune responses. In fact, after completing this manuscript, two in press papers were released where some bacterial components are shown to participate in TLR2-mediated NK activation [34,35]. Our findings furthered these notions by analyzing synthetic Pam2Cys peptides under the knowledge of the structural background of TLR2 [31,32].

A question remaining is why bacteria provide two sorts of lipopeptides with TLR2-activating and –nonactivating properties. So far, we have no experimental finding to sufficiently answer this question, but bacterial infection usually alters host inflammatory milieu and recruits immune competent cells to the lesion [36]. In this context, it is not surprising that Pam2Cys lipopeptides serve as modifiers for host immune response against bacteria. Different responses could be expected to occur with various combinations of Pam2Cys peptides in infectious lesion. Here we demonstrate that

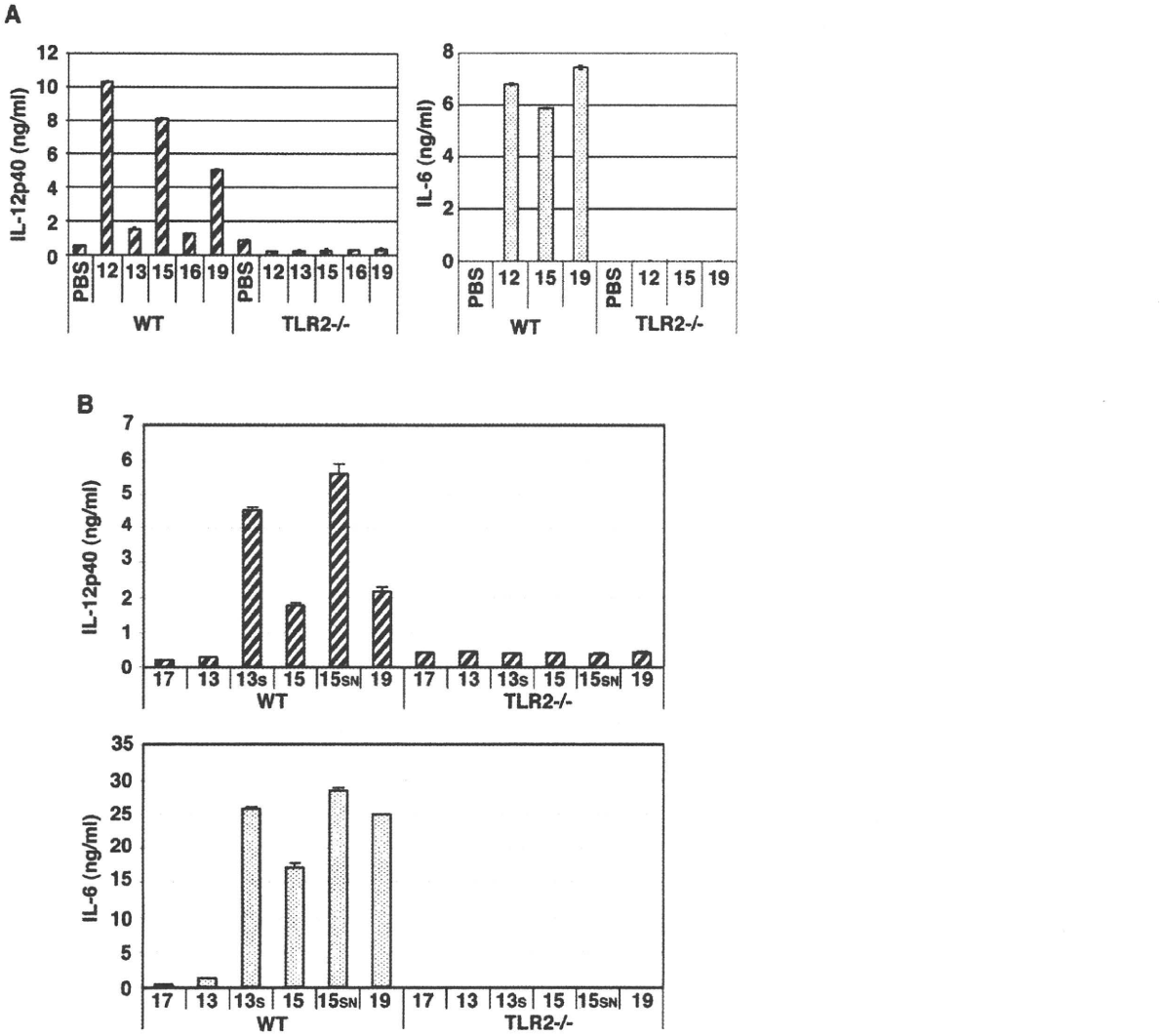

Figure 6. TLR2 agonists in BMDC is crucial for IL-6 and IL-12 production. (A) IL-6 and IL-12p40 production by wild-type but not TLR2−/− BMDC by Pam2Cys stimulation. BMDC prepared from wild-type or TLR2−/− mice were treated with indicated Pam2Cys peptides (100 nM) for 24 h. IL-12p40 and IL-6 concentrations in the supernatants were determined by ELISA. (B) Pam2Cys13(P-S) but not Pam2Cys13 induces IL-6 and IL-12 from BMDC. BMDC prepared from wild-type mice were treated with indicated Pam2Cys peptides (100 nM) for 24 h as in panel A. Cytokines in the supernatants were determined by ELISA. 13S, Pam2Cys13(P-S); 15SN, Pam2Cys15(LI-SN).
doi:10.1371/journal.pone.0012550.g006

NK activation is a phenotype induced by TLR2-activating bacterial lipopeptides, which properties are determined by the peptide sequence of the Pam2Cys. Studies on these functional behaviors of lipopeptide towards mDC and on how TLR signals link NK activation in bacterial infectious diseases will be the next highlight for understanding the importance of early phase of innate cellular response against various bacterial infections.

Materials and Methods

Reagents and antibodies

The following materials were obtained as indicated: Fetal calf serum (FCS) from Bio Whittaker (Walkersville, MD), mouse granulocyte-macrophage colony-stimulating factor (GM-CSF) from PeproTech EC, Ltd (London, UK), polymyxin B from SIGMA-Aldrich (St. Louis, MO), Pam2CSK4 was in part purchased from Amersham Pharmacia Biotech (Piscataway, NJ) and Lympholyte-M from Cedarlane (Ontario, Canada). The enzyme-linked immunosorbent assay (ELISA) kits for mouse (m)IFN-γ from eBioscience (San Diego, CA), and IL-12p40 and IL-6 from Amersham Biosciences.

The following antibodies were used: mAbs against mouse CD11c, NK1.1, CD86, I-Ab, CD25, CD69, DNAM1, CD56 and NKp46 were purchased from BioLegend (San Diego, CA).

Preparation of synthetic peptides

The synthesis of lipopeptides was achieved with a combination of solution- and solid-phase methods [30]. Briefly, for the preparation of the Pam2Cys backbone, the protected cysteine (Fmoc-Cys-OtBu) and the iodide (3-iodopropane-1,2-diol) were

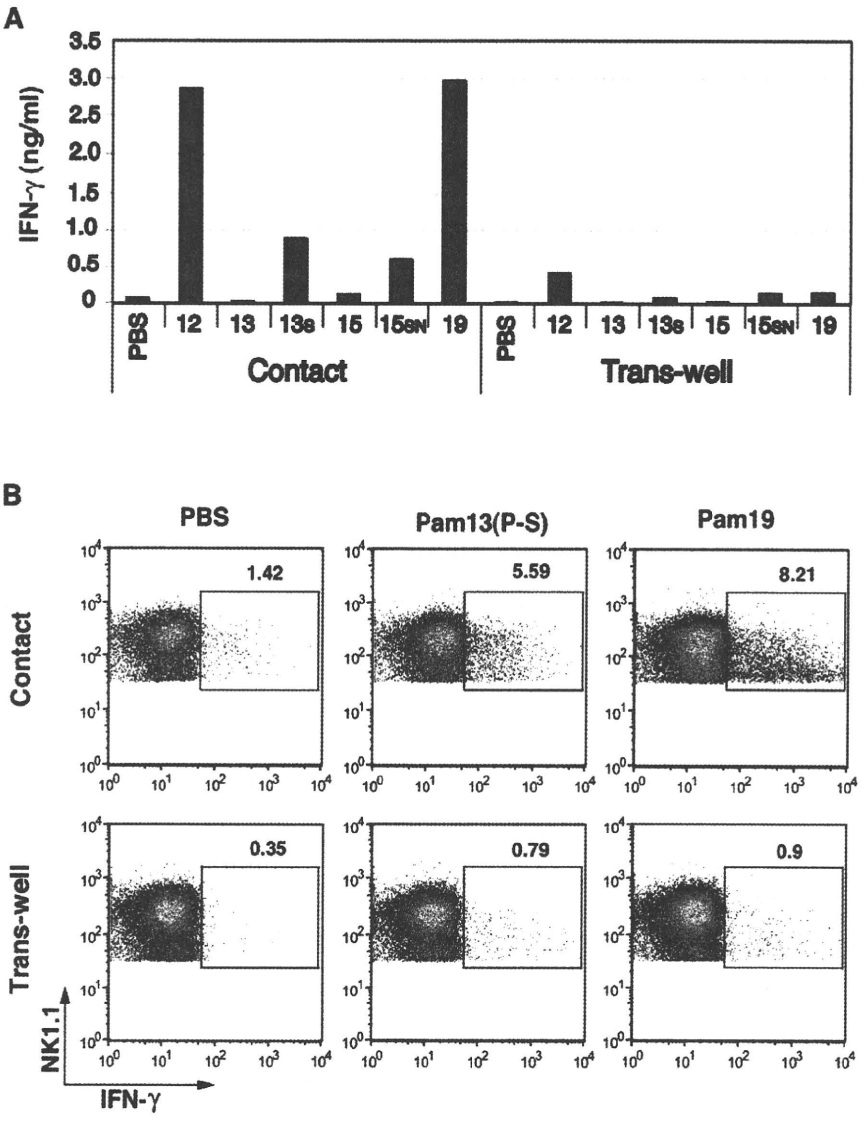

Figure 7. BMDC-NK cell contact induces NK activation. (A) IFN-γ induction by NK cells requires BMDC-NK contact. BMDC prepared from wild-type mice were treated with indicated Pam2Cys peptides (100 nM) for 4 h. Then, BMDC were incubated with naïve NK cells for 24 h at the ratio of 1:2 (left hand bars in Contact). The level of IFN-γ was measured by ELISA. Of note, the sup of the stimulated BMDC was collected and added to cultures of unstimulated BMDC and naïve NK cells, but only a minute level of IFN-γ was detected in the sup (data not shown). The levels of IFN-γ in the same combinations are shown (right hand bars in Trans-well) when stimulated BMDC and NK cells were separated by trans-well. 13S, Pam2Cys13(P-S); 15SN, Pam2Cys15(LI-SN). (B) %IFN-γ-positive NK cells were determined by intracellular staining. Wild-type BMDC prepared from C57BL/6 mice were treated with Pam2Cys13(P-S) peptides (100 nM) for 4 h as in panel A. Then, wild-type NK cells were added to the wells. 20 h after co-culture, breferdin was added to the wells and incubation was continued further for 4 h. NK cell activation was determined by IFN-γ produced in NK cells. %IFN-γ-positive NK cells was determined by FACS.
doi:10.1371/journal.pone.0012550.g007

coupled under basic condition by using Cs_2CO_3 to give Fmoc-Cys(2,3-dihydroxypropyl)-OtBu, and the subsequent acylation and cleavage of the tBu group gave Fmoc-Pam2Cys-OH [37]. The peptide component, which included 16 different peptide sequences from 14 lipoproteins of *S. aureus* NCTC8325, was prepared by using solid-phase synthesis on Wang resin in a similar fashion to Jung's lipopeptide synthesis. Fmoc-Pam2Cys-OH [30,37] was then introduced to the N terminus of the peptides linked to the resin. Subsequent cleavage of the Fmoc group, detachment from the resin, and deprotection of all protecting groups gave the lipopeptides Pam2Cys1–16, and also Pam2CSK4. Pam2CSK and Pam2CSK2 were obtained from Biologica Co. Ltd. Commercial and our synthetic Pam2CSK4 had indistinguishable potential for BMDC maturation and cytokine production (data not shown).

Mouse and cell lines

TLR2 −/−, TLR4 −/−, and MyD88 −/− mice were gifts from Dr. S. Akira (Osaka Univ., Osaka) as previously reported [9].

TICAM-1 (TRIF) −/− and IPS-1 −/− mice were established in our laboratory [4,33]. Female C57BL/6 mice were purchased from Clea Japan (Tokyo). Mice were maintained in our institute under specific pathogen-free conditions. All animal work was performed under guidelines established by the Hokkaido University Animal Care and Use Committee. This study was approved as Analysis of immune modulation by toll-like receptors by this committee. Mice (12 weeks female C57BL/6) were housed four per cage and allowed food and water ad libitum. The Ethics committee in Hokkaido University approved this study (ID number: 08-0243). Animal studies were carefully performed without ethical problems.

B16D8 were established in our laboratory as a subline of the B16 melanoma cell line [38]. This subline was characterized by its low MHC levels with no metastatic properties when injected s.c. into syngeneic C57BL/6 mice [4,33]. HEK293 and B16D8 cell lines were obtained from ATCC (USA). These cell lines were cultured in RPMI 1640/10% FCS.

Preparation of BMDCs and spleen NK cells of mice

Mouse bone marrow-derived DC (BMDC) were prepared as described previously [4]. Spleen NK cells were positively isolated from spleens with DX5 Micro Beads (Miltenyi Biotech) [33]. In experiments requiring high purity NK cells, Thy1.2 beads were additionally used for negative selection according to the Miltenyi's protocol. The purity of NK cells ($DX5^+$ cells) was routinely about 70%. NKT cells might be an only trace constitution of our preparation. $DX5^+$ NK cells were used within 24 h.

Reporter assay

Plasmids (pEFBos) for expression of human TLR1, TLR2, TLR6 and TLR10 were prepared in our laboratory as described previously [39]. HEK293 cells were seeded onto 24-well plates and transfected with 0.1 μg TLR expression vectors, 0.1 μg of ELAM-1, and 0.05 μg of phRL-TK control plasmid using FuGene HD (Roche) according to the manufacturer's instructions. The ELAM-luciferase reporter plasmid was made in our laboratory [13]. After 24 h, the cells were harvested in 50 μl lysis buffer. The luciferase activity was measured using Dual-Luciferase Reporter assay systems (Promega) and was shown as the means ± S.D. of at least three experiments.

Statistical analysis

Student's *t* test was used to examine the significance of the data when applicable in quantitative studies. Differences were considered to be statistically significant when $P<0.05$.

ELISA, Flow cytometric (FACS) analysis of cell surface antigens

The levels of cytokines (IL-6, IL-12p40, IFN-γ etc.) were determined by sandwich ELISA (Amersham Pharmacia Biotech, Buckinghamshire, UK) or the message levels assessed by quantitative PCR [38]. Surface CD25, CD86 and CD69 levels were determined by FACS using specific mAbs. The practical methods for FACS were described previously [40]. Intracellular staining of IFN-γ was peformed with breferdin-treated NK cells as described previously [39]. Trans-well analysis was performed as described previously [40]. Assays were usually performed at least three times in duplicate, otherwise indicated in the legends, and one representative experiment is shown.

Assessment of in vitro cytolytic activity

The cytolytic activity of spleen NK cells was determined by ^{51}Cr assay as described previously [4,33]. NK cells were prepared from the spleen of intact C57BL/6 mice. NK cells were co-cultured with BMDCs at a ratio of 2:1 and 24 h later the mixtures were subdivided to assess NK-mediated cytotoxicity [4]. A B16 subline (D8) or YAC-1 was used as a target cell. Target cells (2×10^3 cells/well) were coincubated with NK cells at the indicated lymphocyte to target (E/T) cell ratio (typically 5, 15 and 30) in U-bottom 96-well plates in a total volume of 200 μl of 0.5% BSA/RPMI-1640 medium at 37°C. Four hours later, the liberated ^{51}Cr in the medium was measured using the scintillation counter. Specific cytotoxic activity was obtained by the formula: Specific cytotoxic activity (%) = [(experimental ^{51}Cr activity - spontaneous ^{51}Cr activity)/(total ^{51}Cr activity − spontaneous ^{51}Cr activity)] ×100. Each experiment was done in triplicate to confirm reproducibility of the results, and representative results are shown. *t* test was used to examine the significance of the data.

Supporting Information

Figure S1 Direct activation of NK cells by stimulation with Pam2Cys12, 18 or 19. Wild-type or TLR2−/− NK cells (5×105 cells/well) were stimulated with indicated Pam2Cys peptides for 24 h. After 24 h, IFN-γ concentrations in the supernatants were measured by ELISA as in Fig. 2A. The IFN-γ concentrations were more than 5-fold lower than those in the mixture of BMDC and NK cells (see Figs. 2A and 3).
Found at: doi:10.1371/journal.pone.0012550.s001 (0.08 MB TIF)

Acknowledgments

We thank Drs. M. Sasai, J. Kasamatsu, H. Takaki, H. Shime, A. H. Hussein, A. Watanabe and H. Oshiumi in our laboratory for their critical discussions. Thanks are also due to Mr. Negishi for his technical assistance. Gifts of TLR2−/− and MyD88−/− mice from Drs. S. Akira are gratefully acknowledged.

Author Contributions

Conceived and designed the experiments: YA TE SY MM TS. Performed the experiments: MA RS YA. Analyzed the data: MA RS TE SY MM TS. Contributed reagents/materials/analysis tools: MH KF YF. Wrote the paper: TS.

References

1. Granucci F, Zanoni I, Ricciardi-Castagnoli P (2008) Central role of dendritic cells in the regulation and deregulation of immune responses. Cell Mol Life Sci 65: 1683–1697.
2. Gerosa F, Baldani-Guerra B, Nisii C, Marchesini V, Carra G, et al. (2002) Reciprocal activating interaction between natural killer cells and dendritic cells. J Exp Med 195: 327–333.
3. Seya T, Matsumoto M (2009) The extrinsic RNA-sensing pathway for adjuvant immunotherapy of cancer. Cancer Immunol Immunother 58: 1175–1184.
4. Akazawa T, Okuno M, Okuda Y, Tsujimura K, Takahashi T, et al. (2007) Antitumor NK activation induced by the Toll-like receptor3-TICAM-1 (TRIF) pathway in myeloid dendritic cells. Proc Natl Acad Sci USA 104: 252–257.
5. Miyake T, Kumagai Y, Kato H, Guo Z, Matsushita K, et al. (2009) Poly I:C-induced activation of NK cells by CD8 alpha+ dendritic cells via the IPS-1 and TRIF-dependent pathways. J Immunol 183: 2522–2528.
6. McCartney S, Vermi W, Gilfillan S, Cella M, Murphy TL, et al. (2009) Distinct and complementary functions of MDA5 and TLR3 in poly(I:C)-mediated activation of mouse NK cells. J Exp Med;Dec. 14.
7. Haller D, Serrant P, Granato D, Schiffrin EJ, Blum S (2002) Activation of human NK cells by staphylococci and lactobacilli requires cell contact-dependent costimulation by autologous monocytes. Clin Diagn Lab Immunol 9: 649–657.
8. Chavakis T, Preissner KT, Herrmann M (2007) The anti-inflammatory activities of *Staphylococcus aureus*. Trends Immunol 28: 408–418.

9. Takeuchi O, Hoshino K, Akira S (2000) Cutting edge: TLR2-deficient and MyD88-deficient mice are highly susceptible to *Staphylococcus aureus* infection. J Immunol 165: 5392–5396.
10. Hashimoto M, Tawaratsumida K, Kariya H, Kiyohara A, Suda Y, et al. (2006) Not lipoteichoic acid but lipoproteins appear to be the dominant immunobiologically active compounds in *Staphylococcus aureus*. J Immunol 177: 3162–3169.
11. Hamerman JA, Ogasawara K, Lanier LL (2004) Cutting edge: Toll-like receptor signaling in macrophages induces ligands for the NKG2D receptor. J Immunol 172: 2001–2005.
12. Fujita M, Into T, Yasuda M, Okusawa T, Hamahira S, et al. (2003) Involvement of leucine residues at positions 107, 112, and 115 in a leucine-rich repeat motif of human Toll-like receptor 2 in the recognition of diacylated lipoproteins and lipopeptides and *Staphylococcus aureus* peptidoglycans. J Immunol 171: 3675–3683.
13. Nakao Y, Funami K, Kikkawa S, Taniguchi M, Nishiguchi M, et al. (2005) Surface-expressed TLR6 participates in the recognition of diacylated lipopeptide and peptidoglycan in human cells. J Immunol 174: 1566–1573.
14. Takeuchi O, Kawai T, Mühlradt PF, Morr M, Radolf JD, et al. (2001) Discrimination of bacterial lipoproteins by Toll-like receptor 6. Int Immunol 13: 933–940.
15. Takeuchi O, Sato S, Horiuchi T, Hoshino K, Takeda K, et al. (2002) Cutting edge: role of Toll-like receptor 1 in mediating immune response to microbial lipoproteins. J Immunol 169: 10–14.
16. Yamamoto M, Sato S, Hemmi H, Sanjo H, Uematsu S, et al. (2002) Essential role for TIRAP in activation of the signalling cascade shared by TLR2 and TLR4. Nature 420: 324–329.
17. Horng T, Barton GM, Flavell RA, Medzhitov R (2001) The adaptor molecule TIRAP provides signalling specificity for Toll-like receptors. Nature 420: 329–333.
18. Iwasaki A, Medzhitov R (2004) Toll-like receptor control of the adaptive immune responses. Nat Immunol 5: 987–995.
19. Matsumoto M, Seya T (2008) TLR3: interferon induction by double-stranded RNA including poly(I:C). Adv Drug Deliv Rev 60: 805–812.
20. Horng T, Barton GM, Medzhitov R (2001) TIRAP: an adapter molecule in the Toll signaling pathway. Nat Immunol 2: 835–841.
21. Oshiumi H, Matsumoto M, Funami K, Akazawa T, Seya T (2003) TICAM-1, an adaptor molecule that participates in Toll-like receptor 3-mediated interferon-beta induction. Nat Immunol 4: 161–167.
22. Martinez J, Huang X, Yang Y (2010) Direct TLR2 signaling is critical for NK cell activation and function in response to vaccinia viral infection. PLoS Pathogen 6: e1000811.
23. Marcenaro E, Ferranti B, Falco M, Moretta L, Moretta A (2008) Human NK cells directly recognize Mycobacterium bovis via TLR2 and acquire the ability to kill monocyte-derived DC. Int Immunol 20: 1155–1167.
24. Akao Y, Ebihara T, Masuda H, Saeki Y, Hazeki K, et al. (2009) Enhancement of antitumor natural killer cell activation by orally administered Spirulina extract in mice. Cancer Sci 100: 1494–1501.
25. Seya T, Shime H, Ebihara T, Oshiumi H, Matsumoto M (2009) Pattern-recognition receptors of innate immunity and their application to tumor immunotherapy. Cancer Sci 101: 313–320.
26. Cerwenka A, Lanier LL (2001) Natural killer cells, viruses and cancer. Nat Rev Immunol 1: 41–49.
27. Hashimoto M, Tawaratsumida K, Kariya H, Aoyama K, Tamura T, et al. (2006) Lipoprotein is a predominant Toll-like receptor 2 ligand in Staphylococcus aureus cell wall components. Int Immunol 18: 355–362.
28. Tawaratsumida K, Furuyashiki M, Katsumoto M, Fujimoto Y, Fukase K, et al. (2009) Characterization of N-terminal structure of TLR2-activating lipoprotein in Staphylococcus aureus. J Biol Chem 284: 9147–9152.
29. Babu MM, Priya ML, Selvan AT, Madera M, Gough J, et al. (2006) A Database of Bacterial Lipoproteins (DOLOP) with Functional Assignments to Predicted Lipoproteins. J Bacteriol 188: 2761–2773.
30. Fujimoto Y, Hashimoto M, Furuyashiki M, Katsumoto M, Seya T, et al. (2009) Innate Immunostimulatory lipopepitdes of *Staphylococcus aureus* as TLR2 ligands; Prediction with mRNA expression, chemical synthesis and immunostimulatory activities. ChemBioChem 10: 2311–2315.
31. Kang JY, Nan X, Jin MS, Youn SJ, Ryu YH, et al. (2009) Recognition of lipopeptide patterns by Toll-like receptor 2-Toll-like receptor 6 heterodimer. Immunity;Nov 18.
32. Jin MS, Kim SE, Heo JY, Lee ME, Kim HM, et al. (2007) Crystal structure of the TLR1-TLR2 heterodimer induced by binding of a tri-acylated lipopeptide. Cell 130: 1071–1082.
33. Ebihara T, Matsumoto M, Seya T (2009) Dendritic cell/NK cell interaction in RNA virus infection. Curr Immunol Rev 5: 200–207.
34. Lindgren A, Pavlovic V, Flach CF, Sjöling A, Lundin S (2010) Interferon-gamma secretion is induced in IL-12 stimulated human NK cells by recognition of Helicobacter pylori or TLR2 ligands. Innate Immun;Feb 3.
35. Mian MF, Lauzon NM, Andrews DW, Lichty BD, Ashkar AA (2010) FimH can directly activate human and murine natural killer cells via TLR4. Mol Ther;May 4.
36. Buwitt-Beckmann U, Heine H, Wiesmüller KH, Jung G, Brock R, et al. (2006) TLR1- and TLR6-independent recognition of bacterial lipopeptides. J Biol Chem 281: 9049–9057.
37. Metzger J, Jung G, Bessler WG, Hoffmann P, Strecker M, et al. (1991) Lipopeptides containing 2-(palmitoylamino)-6,7-bis(palmitoyloxy) heptanoic acid: synthesis, stereospecific stimulation of B-lymphocytes and macrophages, and adjuvanticity in vivo and in vitro. J Med Chem 34: 1969–1974.
38. Tanaka H, Mori Y, Ishii H, Akedo H (1988) Enhancement of metastatic capacity of fibroblast-tumor cell interaction in mice. Cancer Res 48: 1456–1459.
39. Nishiguchi M, Matsumoto M, Takao T, Hoshino M, Shimonishi Y, et al. (2001) Mycoplasma fermentans lipoprotein M161Ag-induced cell activation is mediated by Toll-like receptor 2: role of N-terminal hydrophobic portion in its multiple functions. J Immunol 166: 2610–2616.
40. Tsuji S, Matsumoto M, Takeuchi O, Akira S, Azuma I, et al. (2000) Maturation of human human dendritic cells by cell-wall skeleton of *Mycobacterium bovis* Bacillus Calmette-Guerin: involvement of Toll-like receptors. Infect Immun 68: 6883–6890.

Published November 8, 2010

JEM

Article

Identification of a polyI:C-inducible membrane protein that participates in dendritic cell–mediated natural killer cell activation

Takashi Ebihara,[1] Masahiro Azuma,[1] Hiroyuki Oshiumi,[1] Jun Kasamatsu,[1] Kazuya Iwabuchi,[2] Kenji Matsumoto,[3] Hirohisa Saito,[3] Tadatsugu Taniguchi,[4] Misako Matsumoto,[1] and Tsukasa Seya[1]

[1]Department of Microbiology and Immunology, Hokkaido University Graduate School of Medicine, Kita-ku, Sapporo 060-8638, Japan
[2]Division of Immunobiology, Institute for Genetic Medicine, Hokkaido University, Sapporo, Japan, 060-0815, Japan
[3]Department of Allergy and Immunology, National Research Institute for Child Health and Development, Setagaya-ku, Tokyo 157-8535, Japan
[4]Department of Immunology, Graduate School of Medicine and Faculty of Medicine, University of Tokyo, Bunkyo-ku, Tokyo 113-0033, Japan

In myeloid dendritic cells (mDCs), TLR3 is expressed in the endosomal membrane and interacts with the adaptor toll/interleukin 1 receptor homology domain–containing adaptor molecule 1 (TICAM-1; TRIF). TICAM-1 signals culminate in interferon (IFN) regulatory factor (IRF) 3 activation. Co-culture of mDC pretreated with the TLR3 ligand polyI:C and natural killer (NK) cells resulted in NK cell activation. This activation was triggered by cell-to-cell contact but not cytokines. Using expression profiling and gain/loss-of-function analyses of mDC genes, we tried to identify a TICAM-1–inducing membrane protein that participates in mDC-mediated NK activation. Of the nine candidates screened, one contained a tetraspanin-like sequence and satisfied the screening criteria. The protein, referred to as IRF-3–dependent NK-activating molecule (INAM), functioned in both the mDC and NK cell to facilitate NK activation. In the mDC, TICAM-1, IFN promoter stimulator 1, and IRF-3, but not IRF-7, were required for mDC-mediated NK activation. INAM was minimally expressed on NK cells, was up-regulated in response to polyI:C, and contributed to mDC–NK reciprocal activation via its cytoplasmic tail, which was crucial for the activation signal in NK cells. Adoptive transfer of INAM-expressing mDCs into mice implanted with NK-sensitive tumors caused NK-mediated tumor regression. We identify a new pathway for mDC–NK contact-mediated NK activation that is governed by a TLR signal-derived membrane molecule.

CORRESPONDENCE
Tsukasa Seya:
seya-tu@pop.med.hokudai.ac.jp

Abbreviations used: BMDC, BM-derived DC; IKK, IκB kinase; INAM, IRF-3–dependent NK-activating molecule; IPS-1, IFN promoter stimulator 1; IRF, IFN regulatory factor; mDC, myeloid DC; PRR, pattern recognition receptor; Rae-1, retinoic acid–inducible gene 1; TICAM-1, toll/IL-1 receptor homology domain–containing adaptor molecule 1; TLR, Toll-like receptor.

Natural killer (NK) cells contribute to innate immune responses by killing virus-infected or malignantly transformed cells and by producing cytokines such as IFN-γ and TNF. NK cell activation is determined by a balance of signals from inhibitory and activating receptors. Because ligands of inhibitory receptors include MHC class I and class I–like molecules, the absence of self-MHC expression leads to NK activation (Cerwenka and Lanier, 2001). Approximately 20 receptors contribute to NK activation (Cerwenka and Lanier, 2001; Vivier et al., 2008). When ligands for activating receptors are sufficiently abundant, activating signals overcome inhibitory signals.

There are two currently accepted models for in vivo NK activation. One is that NK cells usually circulate in a naive state and are activated through interaction directly with ligands for pattern recognition receptors (PRRs) expressed by NK cells or interaction with cells that express PRR ligands (Hornung et al., 2002; Sivori et al., 2004). When pathogens enter the host, innate immune sensors, such as Toll-like receptors (TLRs), RIG-I-like receptors,

T. Ebihara and M. Azuma contributed equally to this paper.
T. Ebihara's present address is Howard Hughes Medical Institute, Washington University School of Medicine, St. Louis, MO 63110.

The Rockefeller University Press $30.00
J. Exp. Med. Vol. 207 No. 12 2675-2687
www.jem.org/cgi/doi/10.1084/jem.20091573

Supplemental Material can be found at:
http://jem.rupress.org/content/suppl/2010/11/04/jem.20091573.DC1.html

Published November 8, 2010

NOD-like receptors, and lectin family proteins, which are PRRs, recognize a variety of microbial patterns (pathogen-associated molecular patterns [PAMPs]; Medzhitov and Janeway, 1997). Mouse NK cells express almost all TLRs (TLR1–3, 4, and 6–9), and some of these are directly activated by pathogens with the help of IL-12, IL-18, IFN-γ, and other cytokines (Newman and Riley, 2007). The other is that naive NK cells tend to be recruited to the draining LNs, where they are primed to be effectors with the help of mature myeloid DCs (mDC) and released into peripheral tissues (Fernandez et al., 1999). In this case, mDCs provide direct activating signals to NK cells through cell–cell contact (Gerosa et al., 2002; Akazawa et al., 2007a; Lucas et al., 2007). mDCs also produce proinflammatory cytokines and IFN-α after recognizing PAMPs (Newman and Riley, 2007). In this mDC-mediated NK activation, however, the molecules and mechanisms in mDC that are dedicated to NK activation in vivo remain to be understood.

In this study, we focused on the molecules that are induced in mDC during maturation by exposure to double-stranded (ds) RNA and the molecules involved in priming NK cells for target killing (Akazawa et al., 2007a). dsRNA of viral origin and the synthetic analogue polyI:C induce NK activation in concert with mDC in vivo and in vitro (Seya and Matsumoto, 2009). PolyI:C is recognized by the cytoplasmic proteins RIG-I/MDA5 and the membrane protein TLR3, both of which are expressed in mDC (Matsumoto and Seya, 2008). Although RIG-I and MDA5 in the cytoplasm deliver a signal to the adaptor protein IFN promoter stimulator 1 (IPS-1; also known as MAVS, VISA, and Cardif) on the outer membrane of the mitochondria (Kawai et al., 2005; Meylan et al., 2005; Seth et al., 2005; Xu et al., 2005), TLR3 in the endosomal membrane recruits the adaptor protein toll/IL-1 receptor homology domain–containing adaptor molecule 1 (TICAM-1)/TRIF (Oshiumi et al., 2003a; Yamamoto et al., 2003a). Both adaptor proteins activate TBK1 and/or IκB kinase (IKK) ε, which phosphorylate IFN regulatory factor (IRF) 3 and IRF-7 to induce type I IFN (Sasai et al., 2006). We previously showed that the TLR3–TICAM-1 pathway in mDC participates in inducing anti-tumor NK cytotoxicity by polyI:C (Akazawa et al., 2007a). mDC matured with polyI:C can enhance NK cytotoxicity through mDC-NK cell–cell contact (Akazawa et al., 2007a). Therefore, we hypothesized that an unidentified protein is up-regulated on the cell surface of mDC through activation of the TLR3–TICAM-1 pathway, and this protein enables mDC to interact with and activate NK cells. This is the first study identifying an IRF-3–dependent NK-activating molecule, which we abbreviated INAM. INAM is a TICAM-1–inducible molecule on the cell surface of BM-derived DCs (BMDCs) that activates NK cells via cell–cell contact. Our data imply that mDCs harbor a pathway for driving NK activation that acts in conjunction with dsRNA and TLR3.

RESULTS

TICAM-1/IRF-3 signal in BMDCs augments NK activation

An in vitro system for evaluating NK activation through BMDC-NK contact was established for this study (Fig. 1 A). A mouse melanoma cell subline B16D8, which was established in our laboratory as a low H-2 expressor (Mukai et al., 1999), was used as an NK target. PolyI:C, WT BMDC, and NK cells were all found to be essential for NK-mediated B16D8 cytolysis in the in vitro assay (Fig. 1 A). PolyI:C-mediated NK activation was at baseline levels in a transwell with a 0.4-μm pore, suggesting the importance of direct BMDC-NK contact for this cytolysis induction (Fig. 1 A). When WT BMDCs were replaced with TICAM-1$^{-/-}$ BMDCs in this system, polyI:C-mediated NK activation was partly abolished (Fig. 1 B; and Fig. S1, A and B). TICAM-1 of BMDC was involved in driving NK activation, and ultimately B16D8 cells were damaged by BMDC-derived NK cells (Fig. 1 B). PolyI:C-mediated NK activation occurred even when WT NK cells were replaced with TICAM-1$^{-/-}$ NK cells (Fig. 1 B), which means that NK activation barely depends on the TICAM-1 pathway in NK cells.

PolyI:C-activated splenic NK cells were i.p. injected into B6 mice to kill B16D8 cells ex vivo, which is consistent with previous studies (McCartney et al., 2009; Miyake et al., 2009), and this polyI:C-mediated NK activation was markedly reduced in IPS-1$^{-/-}$ mice established in our laboratory (Fig. S1 C), suggesting that NK cell activation is induced via not only the TICAM-1 pathway but also the IPS-1 pathway, which was largely comparable with previous studies (McCartney et al., 2009; Miyake et al., 2009). IPS-1 in BMDC was more involved in polyI:C-driven NK cytotoxicity than TICAM-1 but almost equally contributed to NK-dependent IFN-γ induction to TICAM-1 in our setting (Fig. S1 B). In addition, the serum level of IL-12p40 in polyI:C-treated mice was largely dependent on TICAM-1 (Fig. S1 D; Kato et al., 2006; Akazawa et al., 2007a). In the supernatant of polyI:C-stimulated BMDC and the serum samples from polyI:C-treated mice, IL-12p70 was not detected by ELISA (unpublished data). These results suggest that polyI:C activates NK cells largely secondary to mDC maturation, which is sustained by the IPS-1 or TICAM-1 pathway of mDC. Even though NK cells express TLR3, they are only minimally activated by polyI:C alone. Signaling by TICAM-1 in BMDC can augment NK cytotoxicity and IFN-γ production via BMDC/NK contact.

The TICAM-1 pathway activates the transcription factor IRF-3. More precisely, exogenous addition of polyI:C can activate endosomal TLR3 and cytoplasmic RIG-I/MDA5. RIG-I/MDA5 assembles the adaptor IPS-1, which in turn recruits the NAP1–IKK-ε–TBK1 kinase complex and activates both IRF-3 and IRF-7 (Fitzgerald et al., 2003; Yoneyama et al., 2004). For this reason, we examined the role of IRF-3 and IRF-7 in BMDC for activation of NK cells by polyI:C. Activation of IRF-3, but not IRF-7, was required for BMDC to induce NK cytotoxicity (Fig. 1 C). IL-2 (Zanoni et al., 2005), IFN-α (Gerosa et al., 2002), and trans-presenting IL-15 (Lucas et al., 2007) induced by BMDC are reported to be key cytokines for BMDC-mediated NK activation in response to polyI:C. However, even with normal levels of IFN-α production and IL-15 expression (Fig. 1, D and E), TICAM-1$^{-/-}$ BMDCs failed to induce full NK cytotoxicity (Fig. 1 B). In contrast, IRF-7$^{-/-}$ BMDCs, which have impaired IFN-α and IL-15

Published November 8, 2010

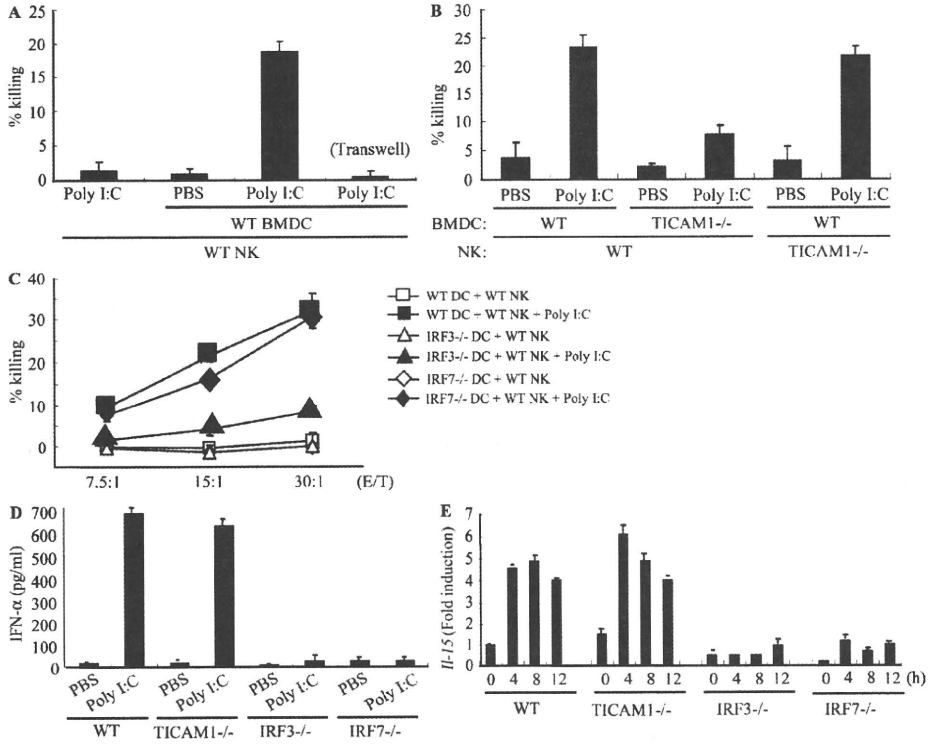

Figure 1. IRF-3 in BMDC controls the capacity to activate NK cells in response to polyI:C. (A and B) WT or TICAM-1$^{-/-}$ NK cells were co-cultured with WT or TICAM-1$^{-/-}$ BMDC in the presence of 10 µg/ml polyI:C for 24 h. NK cytotoxicity against B16D8 was determined by standard ^{51}Cr release assay. E/T = 30. (C) WT NK cells were co-cultured with WT (□, ■), IRF-3$^{-/-}$ (△, ▲), or IRF-7$^{-/-}$ (◇, ◆) BMDC in the presence (■, ▲, ◆) or absence (□, △, ◇) of 10 µg/ml polyI:C for 24 h. NK cytotoxicity against B16D8 was determined by standard ^{51}Cr release assay at the indicated E/T ratio. (D) ELISA of IFN-α in cultures of WT, TICAM-1$^{-/-}$, IRF-3$^{-/-}$, and IRF-7$^{-/-}$ BMDC treated with 10 µg/ml polyI:C for 24 h. (E) Quantitative RT-PCR for IL-15 expression in BMDC stimulated with 10 µg/ml polyI:C. All data are means ± SD of duplicate or triplicate samples from one experiment that is representative of three.

expression, fully activated NK cells (Fig. 1, C–E). Hence, in BDMCs, the TICAM-1–IRF-3 pathway, rather than other cytokines, appears to induce cell surface molecules that mediate BMDC/NK contact and evoke NK cytotoxicity.

Identification of INAM

To identify the NK-activating cell surface molecule on BMDC, we performed microarray analysis on polyI:C-stimulated BMDC prepared from TICAM-1$^{-/-}$ and WT mice. The results yielded nine TICAM-1–inducible molecules with transmembrane motifs (Table S1). Six were induced in an IRF-3–dependent manner, whereas three were still induced in IRF-3$^{-/-}$ BMDC. The NK-activating ability of the products of these genes was investigated by introduction of lentivirus expression vector into IRF-3$^{-/-}$ BMDC. BMDCs with the transduced genes were co-cultured with WT NK cells and polyI:C, and the NK-activating ability was evaluated by determining IFN-γ in the 24-h co-culture. NK cells, but not the gene-transduced BMDCs, produced IFN-γ in the presence of polyI:C. Finally, we identified a tetraspanin-like molecule that satisfied our evaluation criteria (IFN-γ and cytotoxicity) on the mDC-NK activation and named this molecule INAM. INAM clearly differed from other tetraspanins like CD9, CD63, CD81, CD82, and CD151 in the predicted structure. Mouse INAM is a 40–55-kD protein with one N-glycosylation site and possesses four transmembrane motifs (Fig. 2, A and B). Western blotting analysis of INAM-transfected cells under nonreducing conditions showed no evidence of multimers (Fig. 2 B). The N-terminal and C-terminal regions of INAM are in the cytoplasm because anti-Flag antibody did not detect C-terminal Flag-tagged INAM until cells were permeabilized (unpublished data).

Alignment of the predicted amino acid sequence of mouse INAM with that of the human orthologue revealed that the two INAMs shared a 71.7% amino acid identity. INAM is also called FAM26F (Table S1) and is in the FAM26 gene family (Bertram et al., 2008; Dreses-Werringloer et al., 2008). Sequence database searches identified six mouse INAM paralogs. Although FAM26A/CALHM3, FAM26B/CALHM2, and FAM26C/CALHM1 are located on chromosome 19, FAM26D, FAM26E, and FAM26F/INAM are on chromosome 10. Only INAM was inducible with TLR agonists (unpublished data). All FAM26 family proteins have three or four transmembrane motifs predicted by the TMHMM Server (version 2.0). Human CALHM1 has a conserved region (Q/R/N site)

Published November 8, 2010

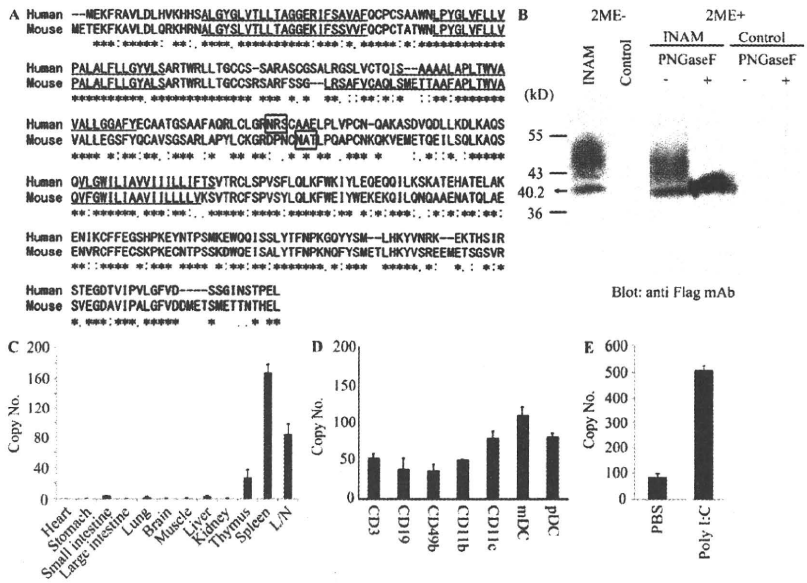

Figure 2. Sequence alignment of INAM and expression of INAM. (A) Sequence alignment of human and mouse INAM. Asterisks, identical residues; double dots, conserved substitutions; single dots, semiconserved substitutions; box, N-glycosylation site; underline, transmembrane motif. (B) Immunoblot analysis of lysates of 293FT cells transfected with plasmid encoding Flag-tagged INAM. PNGase, *N*-glycosidase. 2ME, 2-mercaptoethanol. (C and D) Quantitative RT-PCR for INAM expression in mouse tissue (C) and spleen cells (D). $CD3^+$, $CD19^+$, $DX5^+$, $CD11b^+$, $CD11c^+$, mDC ($CD11c^+PDCA1^+$), and plasmacytoid DC (pDC; $CD11c^+PDCA1^+$) cells were isolated from splenocytes by cell sorting. Data are expressed as copy number per 10^4 copies of HPRT. Data shown are means ± SD of triplicate samples from one experiment that is representative of three. (E) Augmented INAM expression in LN cells after polyI:C stimulation. WT mice were i.p. injected with 100 µg polyI:C or control buffer. After 24 h, inguinal, axillary, and mesenteric LN were harvested and RNA was extracted from the LN cells. The levels of the INAM mRNA were measured by real-time PCR. The results were confirmed in two additional experiments. Data represent mean ± SD.

with ion channel properties at the C-terminal end of the second transmembrane motif that controls cytoplasmic Ca^{2+} levels (Dreses-Werringloer et al., 2008). However, the Q/R/N site was not found in INAM. CALHM1, 2, and 3 are highly expressed in brain. Quantitative RT-PCR revealed that INAM expression was high in spleen and LNs but low in thymus, liver, lung, and small intestine (Fig. 2 C), although expression of the other two FAM26 family members from chromosome 10 was highest in brain (not depicted). All splenocytes examined ($CD3^+$, $CD19^+$, $DX5^+$, $CD11b^+$, $CD11c^+$, mDCs [$CD11c^+$ $PDCA1^-$], and plasmacytoid DCs [$CD11c^-PDCA1^+$]) expressed INAM to some levels (Fig. 2 D). The INAM expression was inducible by polyI:C in LN cells (Fig. 2 E); the induction levels were more prominent in myeloid cells than in lymphocytes in the LNs (Fig. S2 A). $NKp46^+$ and $DX5^+$ NK cells also expressed INAM with low levels and the levels were mildly increased by polyI:C stimulation (Fig. S2 A and not depicted). Notably, only $CD45^+$ cells expressed INAM, which excludes the participation of contaminating stromal cells in the INAM up-regulation (Fig. S2 B).

BMDC INAM activates NK cells

WT and IRF-$7^{-/-}$ BMDCs induced high NK cytotoxicity in response to polyI:C, whereas TICAM-$1^{-/-}$, IPS-$1^{-/-}$, and IRF-$3^{-/-}$ BMDC showed less NK activation (Fig. 1, B and C; and Fig. S1). INAM expression profile by polyI:C stimulation was then examined using WT, IRF-$3^{-/-}$, IRF-$7^{-/-}$, and TICAM-$1^{-/-}$ BMDCs. Stimulation with polyI:C induced INAM at normal levels in IRF-$7^{-/-}$ BMDC but at decreased levels in IRF-$3^{-/-}$ and TICAM-$1^{-/-}$ BMDC (Fig. 3 A). The expression profiles of INAM in polyI:C-stimulated BMDC were in parallel with those inducing NK activation. BMDCs express a variety of TLRs (Iwasaki and Medzhitov, 2004), but other TLR ligands, Pam_3CSK_4 for TLR1/2, Malp2 for TLR2/6, and CpG for TLR9, barely induced INAM on BMDC. High induction of INAM was observed in BMDC stimulated with LPS as well as polyI:C (Fig. 3 B), both of which can activate TICAM-1 to induce IRF-3 and IFN-α activation (Fitzgerald et al., 2003; Oshiumi et al., 2003a,b; Yamamoto et al., 2003a,b). Because INAM is an IFN-inducible gene (Fig. 3 B), INAM induction may be amplified by type I IFNs.

We next examined whether INAM was localized to the cell surface membrane in BMDC. Immunofluorescence analysis showed Flag-tagged INAM on the cell surface of BMDC. Plasma membrane expression of INAM was also confirmed by cell surface biotinylation (Fig. S3). Although the lentivirus inefficiently infected BMDC, GFP expression levels were similar in cells with control virus and those with INAM-expressing virus (Fig. 3 C). Transduction efficiency and expression from the lentivirus vector were adjusted using GFP expression (not depicted), and surface INAM expression was further confirmed with BMDC, NK cells, and INAM-expressing BaF3 (INAM/BaF3) cells, in some cases using polyclonal antibody (Ab) against INAM (Fig. S4).

We then examined whether overexpressing INAM resulted in signaling that directed BMDC maturation and production of cytokines, including IFN-α and IL-12p40, which are reported to enhance NK activity (Gerosa et al., 2002; Sivori et al., 2004; Lucas et al., 2007). The status of INAM-transduced BMDC was assessed by CD86 expression and cytokine production, and no significant differences in these maturation markers were seen in BMDC overexpressing INAM (Fig. S5). In the same setting, no IL-12p70 was

Published November 8, 2010

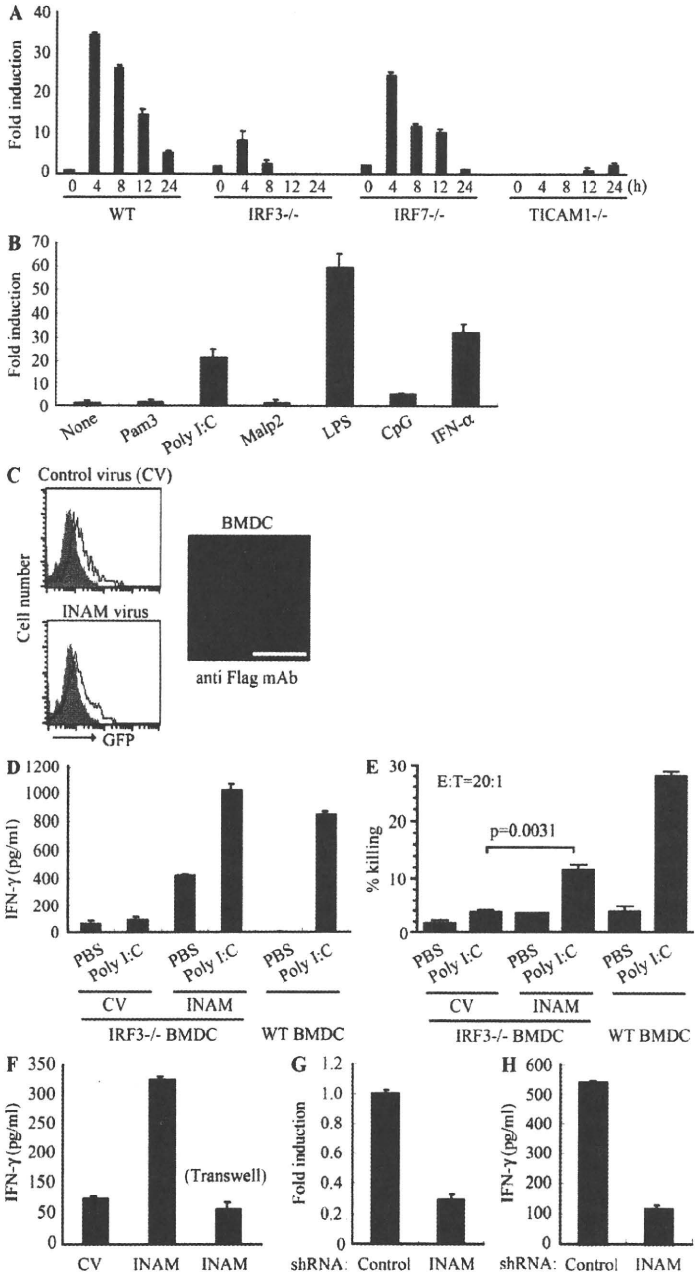

Figure 3. INAM in BMDC participates in DC-mediated NK activation. (A) Quantitative RT-PCR for INAM expression in WT, TICAM-1$^{-/-}$, IRF-3$^{-/-}$, and IRF-7$^{-/-}$ BMDC stimulated with 10 μg/ml polyI:C. (B) Quantitative RT-PCR for INAM expression in WT BMDC stimulated by 100 ng/ml LPS, 10 μg/ml polyI:C, 1 μg/ml Pam3, 100 nM Malp-2, 10 μg/ml CpG, and 2,000 IU/ml IFN-α for 4 h. (C) BMDCs were transduced with Flag-tagged INAM-expressing lentivirus or control lentivirus. GFP expression in the BMDC was determined by flow cytometry, and subcellular localization of INAM was examined by immunofluorescence assay using anti-Flag mAb. Shaded peak, noninfected control; Blank peak, infected BMDC. Bar, 10 μm. (D) ELISA of IFN-γ induced by WT NK cells co-cultured with WT BMDC or IRF-3$^{-/-}$ BMDC transfected with control lentivirus (CV) or INAM-expressing lentivirus (INAM) with/without 10 μg/ml polyI:C. (E) Cytotoxicity against B16D8 by NK cells co-cultured with BMDC transfected with control or INAM-expressing lentivirus with/without 10 μg/ml polyI:C for 24 h. (F) ELISA of IFN-γ induced by WT NK cells co-cultured with IRF-3$^{-/-}$ BMDC transfected with control lentivirus (CV) or INAM-expressing lentivirus (INAM) with 10 μg/ml polyI:C. In some experiments, a transwell was inserted between the INAM-transduced BMDC and NK cells to separate the cells. (G) Quantitative RT-PCR for expression of INAM in BMDC transduced with INAM-shRNA (INAM) or scrambled shRNA (control) and cultured for 48 h. (H) IFN-γ production by WT NK cells determined using ELISA after coculturing with control or the shRNA transfected-BMDC (INAM) and 10 μg/ml polyI:C for 24 h. All data shown are means ± SD of triplicate samples from one experiment that is representative of three.

detected by ELISA (unpublished data). In addition, polyI:C-mediated NK activation occurred in BMDC expressing an INAM mutant lacking the cytoplasmic C-terminal region (193–327 aa; Fig. 4, A and B), excluding the participation of the cytoplasmic region in BMDC maturation signaling.

To investigate whether INAM could reconstitute NK-activating ability in IRF-3$^{-/-}$ BMDC, we transduced INAM into IRF-3$^{-/-}$ BMDC and incubated BMDC with NK cells. Overexpression of INAM in IRF-3$^{-/-}$ BMDC induced NK IFN-γ production and NK cytotoxicity against B16D8, and this NK activation was further enhanced by the addition of polyI:C (Fig. 3, D and E). Thus, polyI:C may also work for NK activation. Direct cell–cell contact with NK cells was required for INAM in IRF-3$^{-/-}$ BMDC to function on enhancing NK activity (Fig. 3 F).

We further confirmed this issue using WT BMDC by shRNA gene silencing. We silenced the INAM gene in BMDC using the lentiviral vector pLenti-dest-IRES-hrGFP and monitored expression by GFP. Because transfection efficiency was relatively high in this case compared with that shown in Fig. 3 C, the expression level of INAM had decreased by ~75% in WT BMDC compared with the nonsilenced control (Fig. 3 G and Fig. S6 A). Although the level of the endogenous INAM protein was not very high, we confirmed that INAM protein was also decreased by shRNA with immunoblotting using anti-INAM pAb (Fig. S7 A). PolyI:C response of BMDC-inducible cytokines tested was not altered by INAM silencing in BMDC (Fig. S6 B). Yet this INAM RNA interference caused a significant decrease in NK cell IFN-γ production after co-culture of the INAM knockdown BMDCs and WT NK cells with polyI:C (Fig. 3 H). Collectively, these results indicate that INAM is downstream of IRF-3 in BMDC and is involved in the activation of NK cells by BMDC.

Published November 8, 2010

Using an INAM-expressing stable BaF3 cell line (INAM/BaF3), we tested the possibility that INAM is an activating ligand for NK cells. As a positive control, we produced a stable BaF3 cell line expressing Rae-1α (Fig. 5 A) which is a ligand for the NK-activating receptor NKG2D (Cerwenka et al., 2000). Although Rae-1α/BaF3 cells were easily damaged by IL-2–activated NK cells, INAM/BaF3 cells were not (Fig. 5 B). In this context, addition of IRF-3$^{-/-}$ BMDC to this culture with BaF3 and NK cells led to slight augmentation of IFN-γ induction irrespective of the presence of INAM on BaF3 cells (Fig. 5 C), and β2-microglobulin$^{-/-}$ BMDC barely affected the IFN-γ level (not depicted). These results suggest that an INAM-containing molecular matrix, rather than INAM alone, acts toward NK cells. Alternatively, INAM may selectively function with specific mDC molecules to activate NK cells.

INAM on NK cells is required for efficient NK activation

mDCs were previously shown to be required for efficient NK activation in vivo and in vitro (Akazawa et al., 2007a). We found that INAM was minimally present in BMDCs and NK cells and that polyI:C acts on both (Figs. S2 A; and Fig 3, D and E). Tetraspanin-like molecules tend to work as scaffolds for heteromolecular complexes that contain molecules functioning in a cis- or trans-adhesion manner to exert intercellular or extracellular functions. Thus, the function of INAM may not be confined to mDC, so we studied the function of INAM on NK cells. In NK cells, INAM was also inducible by polyI:C (Fig. 6 A and Fig. S2 A), and the induction of INAM was abrogated completely in IRF-3$^{-/-}$ NK cells and moderately in TICAM1$^{-/-}$ NK cells (Fig. 6 B). This suggests that polyI:C also acts on NK cells and induces INAM through IPS-1/IRF-3 activation when NK cells are co-cultured with BMDC and polyI:C.

To investigate whether INAM induced in NK cells is associated with BMDC-mediated NK activation, we performed the following experiments (Fig. 6 C). INAM-transduced IRF-3$^{-/-}$ BMDCs were incubated with polyI:C for 4 h, and then the aliquot was mixed with WT NK cells in the presence of polyI:C (Fig. 6 C, left two lanes). A moderate increase of IFN-γ was observed as in Fig. 3 D. In the remainder,

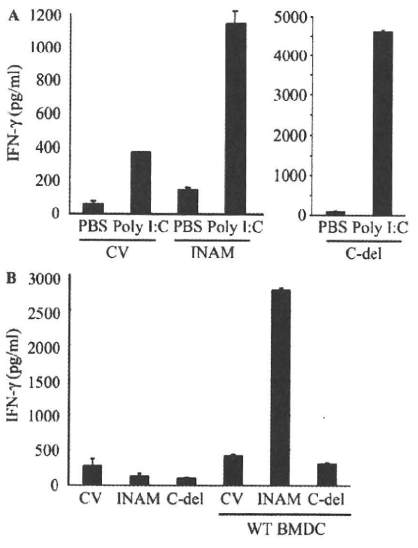

Figure 4. Role of the cytoplasmic tail of INAM. (A) The C-terminal region of INAM was not required for BMDC-mediated NK activation. ELISA of IFN-γ by WT NK cells co-cultured with IRF-3$^{-/-}$ BMDCs transfected with control lentivirus (CV) or a lentivirus expressing intact INAM or a mutant INAM lacking the C-terminus (C-del INAM) with/without 10 μg/ml polyI:C. Data shown are means ± SD of triplicate samples from one experiment representative of three. (B) The cytoplasmic tail of INAM is indispensable for NK IFN-γ induction. INAM or C-del INAM (A) was expressed on IRF-3$^{-/-}$ NK cells. The INAM (or C-del INAM)-expressing IRF-3$^{-/-}$ NK cells were incubated with or without WT BMDC for 24 h. IFN-γ levels in the supernatants were determined by ELISA. One representative result out of several similar experiments is shown. Data represent mean ± SD.

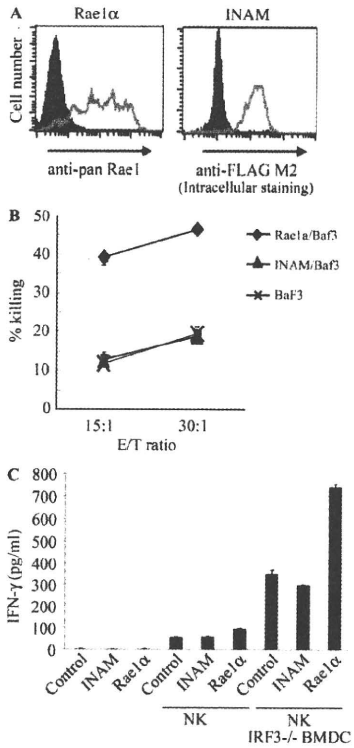

Figure 5. INAM is not an NK-activating ligand. (A) Flow cytometry for Rae-1 and Flag-tagged INAM in stable BaF3 lines. Shaded peak, untransfected control BaF3 staining with anti-pan-Rae-1 Ab or anti-Flag M2 antibody; open peak, stable Rae-1α/BaF3 or stable Flag-tagged INAM/BaF3 staining with anti-pan-Rae-1 antibody or anti-Flag M2 antibody. (B) Cytotoxicity against control BaF3, Rae-1α/BaF3, and INAM/BaF3 by NK cells treated with 1,000 IU/ml IL-2 for 3 d. Data shown are means ± SD of triplicate samples from one experiment representative of three. (C) NK activation is augmented by coexistent BMDC irrespective of INAM expression. NK cells were cultured with 1,000 IU/ml IL-2 for 3 d. 2 × 10^5 NK cells, 10^5 BaF3 cells, and 10^5 IRF-3$^{-/-}$ BMDCs were co-cultured in 200 μl/well and IFN-γ in the supernatants were measured by ELISA. Data show one of two similar experimental results. Data represent mean ± SD.

Published November 8, 2010

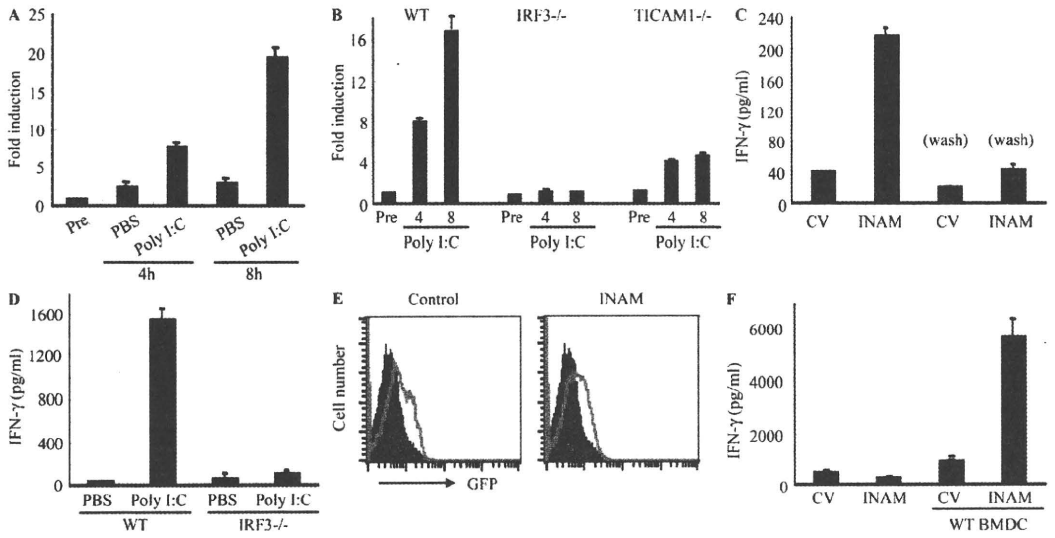

Figure 6. INAM on NK cells contributes to efficient NK activation mediated by mDC. (A and B) Quantitative RT-PCR for INAM expression in WT, TICAM1$^{-/-}$, or IRF-3$^{-/-}$ NK cells stimulated with 50 µg/ml polyI:C. Data shown are means of duplicate or triplicate samples from one experiment that is representative of three. (C) IRF-3$^{-/-}$ BMDCs were transfected with control lentivirus (CV) or INAM-expressing lentivirus (INAM) before treatment with 10 µg/ml polyI:C for 4 h. BMDCs in some wells were washed to remove polyI:C before WT NK cells were added (Wash). IFN-γ production by NK cells was determined by ELISA after 24 h of culture. Data show one of two similar experimental results. (D) ELISA of IFN-γ in co-culture of WT or IRF-3$^{-/-}$ NK cells and WT BMDC with/without 10 µg/ml polyI:C. (E and F) NK cells were transfected with control lentivirus or INAM-expressing lentivirus and cultured with 500 IU/ml IL-2 for 3 d. After determining transfection efficiency by GFP intensity using flow cytometry, cells were cultured with/without BMDC for 24 h and IFN-γ production in the supernatant determined by ELISA. Shaded peak, noninfected control; open peak, infected BMDC. All data are means ± SD of triplicate samples from one experiment that is representative of three.

we washed polyI:C out and cultured the cells with WT NK cells (Fig. 6 C, right two lanes). Under these conditions, in which polyI:C acted not on NK cells but only on BMDC, little NK activation was observed (Fig. 6 C). Furthermore, IRF-3$^{-/-}$ NK cells produced little IFN-γ when co-cultured with WT BMDC and polyI:C (Fig. 6 D). INAM-overexpressing IRF-3$^{-/-}$ BMDC required IRF-3 in NK cells for efficient BMDC-mediated production of IFN-γ from NK cells (Fig. 6 D). We next transduced INAM into IRF-3$^{-/-}$ NK cells using a lentivirus (INAM/pLenti-IRES-hrGFP) to reconstitute NK IFN-γ–producing activity. After many trials with various setting conditions, we found that ~15% of the DX5^{+} NK cell population was both GFP-positive and stained with anti-FLAG mAb when treated with high doses of INAM-expressing lentivirus vector (Fig. S7 B). When IRF-3$^{-/-}$ NK cells were infected with smaller amounts of INAM-expressing lentiviral vector and cultured for 3 d with high concentrations of IL-2 (500 IU/ml), slight but significant GFP expression was confirmed by FACS (Fig. 6 E). Then, the INAM-transduced IRF-3$^{-/-}$ NK cells were co-cultured with WT BMDC. The IRF-3$^{-/-}$ NK cells with INAM expression secreted IFN-γ at significantly higher levels than controls in the presence of WT BMDC (Fig. 6 F). These data indicate that INAM is induced by polyI:C through IRF-3 activation, not only in BMDCs but also in NK cells, and that INAM on NK cells synergistically works with INAM on BMDC for efficient NK cell activation. Both INAMs on BMDC and NK cells are essential for BMDC-mediated NK activation.

We next checked the function of the C-terminal stretch of INAM in NK activation. Although intact INAM works in NK cells to produce IFN-γ in response to BMDC (Fig. 6 F), introduction of C-del INAM into IRF-3$^{-/-}$ NK cells did not result in high induction of IFN-γ in response to BMDC (Fig. 4 C). Thus, INAM participates in NK activation through its cytoplasmic regions, which has no significant role in BMDC for NK activation.

Anti-tumor NK activation via INAM-expressing BMDCs in vivo

mDC-mediated NK activation induces anti-tumor NK cells, which cause regression of NK-sensitive tumors (Kalinski et al., 2005; Akazawa et al., 2007a). We tested the in vivo function of INAM-expressing BMDC using B16D8 tumor-bearing mice. BMDCs were used 24 h after transfection with either INAM/pLenti-IRES-hrGFP or control pLenti-IRES-hrGFP and injected twice a week s.c. around a preexisting tumor in tumor-implanted mice, beginning 11–13 d after tumor challenge. INAM-expressing BMDC significantly retarded tumor growth (Fig. 7 A). Tumor retardation was abrogated by depletion of NK1.1-positive cells (Fig. 7 B). Thus, INAM expression on BMDC contributed to anti-tumor NK activation in vivo.

When the control or INAM-expressing IRF-3$^{-/-}$ BMDCs were co-cultured with WT NK cells in vitro, there was no induction of the mRNA of TRAIL and granzyme B in

Published November 8, 2010

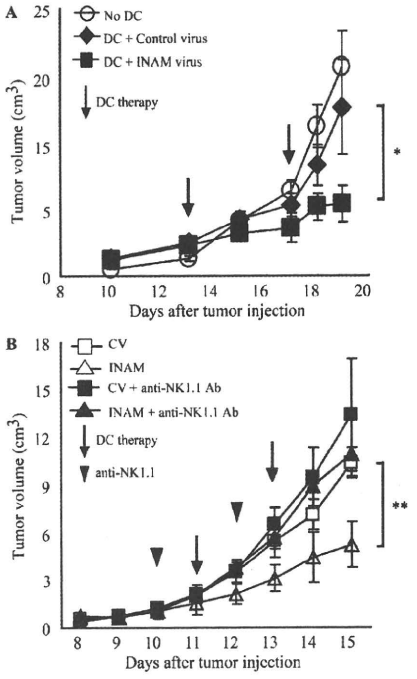

Figure 7. INAM on BMDC retarded B16D8 tumor growth in an NK-dependent manner. (A) Tumor volume after DC therapy using BMDC expressing INAM. B16D8 cells were s.c. injected into C57BL/6 mice and, 11–13 d later, medium only (○) or BMDC (10^6/mouse) transfected with control lentivirus (◆) or those with INAM-expressing lentivirus (■) were administered s.c. near the tumor at the time indicated by the open arrow. *, P = 0.043. Data represent mean ± SD. (B) Abrogation of INAM-dependent tumor regression by administration of NK1.1 Ab. For depletion of NK cells, antiNK1.1 mAb was injected i.p. 1 d before treatment of BMDC (arrowheads). Tumor volume in every mouse group was sequentially monitored. Data represent mean ± SD (n = 3) and are representative of two experiments. Statistical analyses were made with the Student's t test. **, P = 0.017.

NK cells (Fig. 8 A). TRAIL and granzyme B were induced in NK cells by the addition of polyI:C to the mixture, and INAM expression in BMDC up-regulated mRNA levels of TRAIL and granzyme B (Fig. 8 A). In vivo administration studies were performed with polyI:C-treated WT BMDC or INAM-expressing IRF-$3^{-/-}$ BMDC to test their ability to up-regulate the mRNA levels of TRAIL and granzyme B in NK cells in draining LN (Fig. 8 B). INAM-expressing IRF-$3^{-/-}$ BMDC showed comparable abilities to up-regulate the killing effectors with polyI:C-treated BMDC (Fig. 8 B). Collectively, INAM has therapeutic potential for NK-sensitive tumors by activating NK cells.

DISCUSSION

Previous studies demonstrated that mDC–NK interaction leads to direct NK activation and damages NK target cells in vitro (Gerosa et al., 2002; Sivori et al., 2004; Akazawa et al., 2007a; Lucas et al., 2007). In addition, mDCs initiate NK cell–mediated innate anti-tumor immune responses in vivo (Kalinski et al., 2005; Akazawa et al., 2007a,b). Systemic administration of polyI:C unequivocally results in activation of peripheral NK cells (Lee et al., 1990; Sivori et al., 2004; Akazawa et al., 2007a). Although the molecular mechanism by which mDCs prime NK cells was still unclear, the TICAM-1 pathway and IPS-1 pathway have been reported to participate in polyI:C-mediated mDC maturation that drives NK activation (Akazawa et al., 2007a; McCartney et al., 2009; Miyake et al., 2009). We have shown in an earlier study that mDCs disrupted in the TLR3–TICAM-1 pathway abrogate NK cell activation (Akazawa et al., 2007a,b). In TICAM-$1^{-/-}$ mice, NK-sensitive implant tumors grew as well as those in WT mice depleted of NK cells (Akazawa et al., 2007a). mDCs gain high anti-tumor potential against B16D8 implant tumors through lentiviral transfer of TICAM-1, which is attributable to NK activation (Akazawa et al., 2007a). We further showed that TICAM-1 is a critical molecule for mDC to induce NK cell IFN-γ, as well as IPS-1, and participates in driving NK cytotoxicity to a lesser extent than IPS-1. In this paper, we clarified a molecular mechanism by which mDCs immediately promote NK cell functions in vitro and in vivo.

Our findings showed that IRF-3 is the transcription factor that is downstream of TICAM-1 responsible for maturing mDC to an NK-activating phenotype. We discovered that INAM, a membrane-associated protein, is up-regulated on the surface of mDC by polyI:C stimulation and activates NK cells via cell–cell contact. Furthermore, we found that NK cells also express INAM on their cell surface after polyI:C stimulation. mDC–NK activation by polyI:C can be reproduced with INAM-transduced mDC and NK cells, and adoptive transfer experiments show that INAM-overexpressing mDC may have therapeutic potential against MHC-low melanoma cells in an NK-dependent manner. These functional properties of INAM-expressing mDC fit the model of mDC priming NK activation. Ultimately, INAM appears to be the key molecule in the previously reported mechanism of mDC–NK contact activation.

After the submission of this manuscript, two papers were published that found that the MDA5–IPS-1 pathway in mDC is more important for driving NK activation, particularly in vivo (McCartney et al., 2009; Miyake et al., 2009). Our data also support this point using the IPS-$1^{-/-}$ mice we established (Fig. S1). However, polyI:C, when i.v. administered into mice, may stimulate other systemic cells in addition to $CD8^+$ mDC in vivo (McCartney et al., 2009). The difference among the two (McCartney et al., 2009; Miyake et al., 2009) and this study may be attributed to the setting conditions, which are not always comparable. Moreover, it remains to be settled whether TICAM-1 and IPS-1 take the same INAM complex as a common NK activator in mature mDC and whether TLR3 (or MDA5) KO is equivalent to TICAM-1 (or IPS-1) KO in the mDC–NK activation model. In either case, however, up-regulation of mDC TICAM-1–mediated NK cytotoxicity and IFN-γ induction are feasible with polyI:C under three different conditions (Akazawa et al., 2007a; McCartney et al., 2009; Miyake et al., 2009). Our results infer that INAM participates in at least these mDC–NK interactions.

Published November 8, 2010

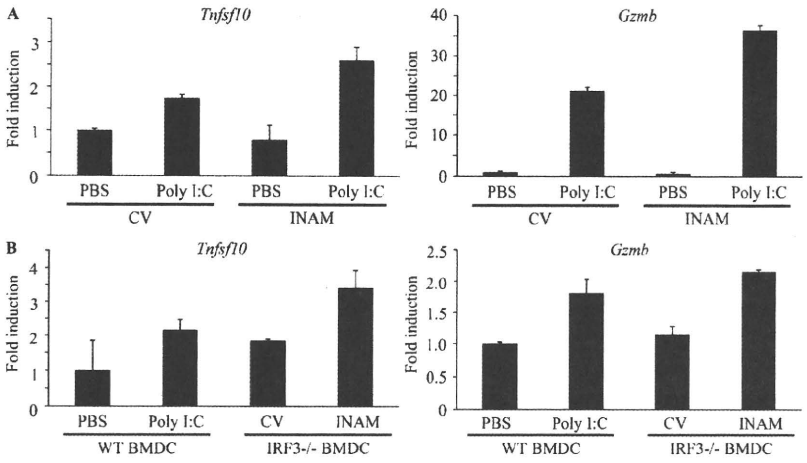

Figure 8. INAM-mediated induction of TRAIL and granzyme B in BMDC. (A) In vitro induction of TRAIL (Tnfsf10) and granzyme B (Gzmb) mRNA by INAM-expressing BMDC. BMDCs (IRF-3$^{-/-}$) were infected with INAM-expressing virus or CV as in Fig. S4. After 24 h, the BMDCs (IRF-3$^{-/-}$) were incubated with WT NK cells at DC/NK = 1:2. 8 h later, DX5^{+} cells were collected by FACS sorting and their RNA was extracted to determine the mRNA levels of the indicated genes. A representative result of three similar experiments are shown. (B) In vivo induction of TRAIL and granzyme B mRNA by INAM-expressing BMDC. WT BMDCs were stimulated with 10 μg/ml polyI:C or medium only. IRF-3$^{-/-}$ BMDCs were infected with CV or INAM-expressing vector. These BMDCs were allowed to stand for 24 h and then 5 × 10^{5} cells were injected into footpads of WT mice. After 48 h, DX5^{+} cells were collected from the inguinal LN by FACS sorting. RNA of the cells was extracted and the levels of the indicated mRNA were determined by real time PCR. Data show one of two experiments with similar results. Data in A and B represent mean ± SD.

PolyI:C activates IRF-3 through the two pathways involving the adaptors IPS-1 and TICAM-1 (Yoneyama et al., 2004; Kato et al., 2006; Matsumoto and Seya, 2008). The two pathways share the complex of IRF-3–activating kinase, NAP1, IKK-ε, and TBK1 that is downstream of adaptors (Sasai et al., 2006). Nevertheless, these pathways are capable of inducing several genes unique to each adaptor. Although IFN-α production by in vivo administration of polyI:C is largely dependent on the IPS-1 pathway, IL-12p40 is mainly produced by the TICAM-1 pathway (Kato et al., 2006). Therefore, it is not surprising that INAM induction is predominant in the TICAM-1 pathway in polyI:C-stimulated BMDC (Fig. 3 A). What happens in IRF-7$^{-/-}$ BMDCs in terms of INAM induction and what mechanism sustains BMDC IPS-1–mediated or MyD88-mediated activation of NK cells (Azuma et al., 2010) will be issues to be elucidated in the future.

Although IRF-3–regulated cell surface INAMs are required for efficient interaction between BMDC and NK cells, the mechanism by which forced expression of INAM causes signaling for BMDC maturation is still unknown. Although the NK-activating capacity of BMDCs is usually linked to their maturation, neither cytokines in NK activation, including IFN-α and IL-12p70, nor costimulators, such as CD40 and CD86, were specifically induced in mDC by INAM expression (Fig. S5). INAM has a C-terminal cytoplasmic stretch (Fig. 4 A), and we tested the function of this region by a deletion mutant (C-del INAM). This region in BMDC barely participates in driving NK activation because no decrease of IFN-γ induction by NK cells was observed with IRF-3$^{-/-}$ BMDC supplemented with C-del INAM compared with control INAM. Thus far, no significant signal alteration has been detected in BMDC supplemented with INAM by lentivirus.

In contrast, INAM-transduced IRF-3$^{-/-}$ NK cells produced IFN-γ in concert with BMDCs like WT NK cells (Fig. 6 F). So far we have no evidence suggesting that this kind of INAM overexpression is actually occurring in vivo. However, introduction of C-del INAM into IRF-3$^{-/-}$ NK cells did not result in high induction of IFN-γ in response to BMDC (Fig. 4 C). Together with the data on INAM expression in BMDC, this infers that the INAM cytoplasmic region signals for NK activation in NK cells. The one-way role of the cytoplasmic tail in NK activation will be an issue for further analysis.

In this study, IL-15 was found to be up-regulated by polyI:C in BMDC. The remaining NK activity in the resting population of NK cells co-cultured with TICAM-1$^{-/-}$ BMDC and polyI:C (Fig. 1 B) suggests that IL-15 has some effect in our system, and other studies suggest this as well (Ohteki et al., 2006; Brilot et al., 2007; Lucas et al., 2007; Huntington et al., 2009). However, we did not observe decreased IL-15 expression in the TICAM-1$^{-/-}$ BMDC that could not activate NK cells (Fig. 1 E). Several molecules, such as B7-H6/NKp30 (Brandt et al., 2009), CD48/2B4 (Kubin et al., 1999), and NKG2D ligands/NKG2D (Cerwenka et al., 2000), have been identified as ligand/receptor molecules in mDC–NK reciprocal activation by in vitro co-culture. In in vitro co-culture systems (Fig. S1), the IPS-1 pathway in BMDC has a pivotal role in not only type I IFN but also IL-15 induction. INAM identified in this paper serves a unique function in the in vivo induction of NK activation and may offer a tool to investigate the reported mDC-mediated NK activation.

Rae-1 was reported as a molecule with MHC-like structure (Zou et al., 1996) and later identified as a mouse NKG2D ligand (Cerwenka et al., 2000). Although Rae-1 is a GPI-anchored protein with no cytoplasmic sequences (Nomura et al., 1996), it can act as an NK-activating ligand (Cerwenka et al., 2000, 2001; Masuda et al., 2002). Mouse BaF3 cells become NK-sensitive after forced expression of Rae-1α (Masuda et al., 2002). Actually, mouse macrophages induce Rae-1 expression in response to TLR stimuli (Hamerman et al., 2004). In contrast,